VTRC Virginia Transportation Research Council

We Bring Innovation to Transportation

Innovative Coating Removal Techniques for Coated Bridge Steel

http://www.virginiadot.org/vtrc/main/online_reports/pdf/20-r1.pdf

James M. Fitz-Gerald, Ph.D.
Professor of Materials Science and Engineering, University of Virginia

Sean R. Agnew, Ph.D.
Professor of Materials Science and Engineering, University of Virginia

William Moffat
Graduate Student, University of Virginia

Stephen R. Sharp, Ph.D., P.E.
Senior Research Scientist, Virginia Transportation Research Council

James S. Gillespie
Senior Research Scientist, Virginia Transportation Research Council

Donald R. Becker
Corrosion and Coatings Program Manager, Turner-Fairbank Highway Research Center

Rongtang Liu, Ph.D., P.E.
Engineering Lab Manager, SES Group and Associates

Arthur Runion
Lab Research Assistant, SES Group and Associates

Final Report VTRC 20-R1

VIRGINIA TRANSPORTATION RESEARCH COUNCIL
530 Edgemont Road, Charlottesville, VA 22903-2454
vtrc.virginiadot.org

Standard Title Page - Report on Federally Funded Project

1. Report No.: FHWA/VTRC 20-R1	2. Government Accession No.:	3. Recipient's Catalog No.:
4. Title and Subtitle: Innovative Coating Removal Techniques for Coated Bridge Steel		5. Report Date: August 2019
		6. Performing Organization Code:
7. Author(s): James M. Fitz-Gerald, Ph.D., Sean R. Agnew, Ph.D., William Moffat, Stephen R. Sharp, Ph.D., P.E., James S. Gillespie, Donald R. Becker, Rongtang Liu, Ph.D., P.E., and Arthur Runion		8. Performing Organization Report No.: VTRC 20-R1
9. Performing Organization and Address: Virginia Transportation Research Council 530 Edgemont Road Charlottesville, VA 22903		10. Work Unit No. (TRAIS):
		11. Contract or Grant No.: 109552
12. Sponsoring Agencies' Name and Address: Virginia Department of Transportation 1401 E. Broad Street Richmond, VA 23219 Federal Highway Administration 400 North 8th Street, Room 750 Richmond, VA 23219-4825		13. Type of Report and Period Covered: Final
		14. Sponsoring Agency Code:

15. Supplementary Notes:
This is an SPR-B report.

16. Abstract:

The purpose of this study was to determine if the use of a laser ablation coating removal (LACR) system would provide the Virginia Department of Transportation (VDOT) with an acceptable new alternative for removing existing coatings. In this study, the LACR process was documented in the laboratory and in the field to determine the feasibility of implementing LACR for VDOT bridges. All LACR work was performed on actual structural steel features from Virginia bridges. Industrial hygiene surveys of the LACR process were used to determine the environmental and worker safety of LACR. Laboratory material analysis of samples evaluated the effects on the properties of steel bridge components.

This work led to the following conclusions.

- LACR effectively removes the coatings investigated, including lead-based coatings. Although microscopic investigation revealed that small coating particles remained on the surface after cleaning (which were not visible to the naked eye), this did not appear to affect subsequent coating adhesion adversely.
- The coating adhesion of LACR surfaces, tested by two independent laboratories, is acceptable.
- LACR does not detrimentally affect the mechanical properties of the ASTM A36 structural steel examined in this study. The tensile yield strength, ultimate tensile strength, ductility, and fatigue strength were on parity with expected values.
- The industrial hygiene study results showed that the engineering controls associated with the LACR system maintained potential exposures to hazardous air pollutants for the laser operator well below the current Occupational Safety and Health Administration's permissible exposure limit and action limit for each constituent sampled within a worker's breathing zone and adjacent work area. This could provide a potential cost benefit, since LACR does not require the type of containment that traditional grit-blasting approaches require.
- Similar to traditional coating removal technologies, the waste generated by LACR was classified as a regulatory hazardous waste; appropriate personal protective equipment must be worn during management of the waste material and filters.
- In the field, the LACR system was effective on bridge beam ends and bulk heads in open spaces but was more problematic in tight spaces where the geometry limited access to the coated surface. The team did observe, but were unable to test in detail, other LACR systems that were smaller, lighter weight, and more powerful.

LACR can be employed as a lead-based coating removal technique in preparation for other manufacturing processes, such as cutting or welding routinely performed by VDOT. Such applications would not necessarily require high productivity rates or access to tight spaces.

17 Key Words: bridge, coating, hot work, lead, laser ablation coating removal, LACR	18. Distribution Statement: No restrictions. This document is available to the public through NTIS, Springfield, VA 22161.

19. Security Classif. (of this report): Unclassified	20. Security Classif. (of this page): Unclassified	21. No. of Pages: 72	22. Price:

FINAL REPORT

INNOVATIVE COATING REMOVAL TECHNIQUES FOR COATED BRIDGE STEEL

James M. Fitz-Gerald, Ph.D.
Professor of Materials Science and Engineering, University of Virginia

Sean R. Agnew, Ph.D.
Professor of Materials Science and Engineering, University of Virginia

William Moffat
Graduate Student, University of Virginia

Stephen R. Sharp, Ph.D., P.E.
Senior Research Scientist, Virginia Transportation Research Council

James S. Gillespie
Senior Research Scientist, Virginia Transportation Research Council

Donald R. Becker
Corrosion and Coatings Program Manager, Turner-Fairbank Highway Research Center

Rongtang Liu, Ph.D., P.E.
Engineering Lab Manager, SES Group and Associates

Arthur Runion
Lab Research Assistant, SES Group and Associates

In Cooperation with the U.S. Department of Transportation
Federal Highway Administration

Virginia Transportation Research Council
(A partnership of the Virginia Department of Transportation
and the University of Virginia since 1948)

Charlottesville, Virginia

August 2019
VTRC 20-R1

DISCLAIMER

The contents of this report reflect the views of the authors, who are responsible for the facts and the accuracy of the data presented herein. The contents do not necessarily reflect the official views or policies of the Virginia Department of Transportation, the Commonwealth Transportation Board, or the Federal Highway Administration. This report does not constitute a standard, specification, or regulation. Any inclusion of manufacturer names, trade names, or trademarks is for identification purposes only and is not to be considered an endorsement.

ABSTRACT

The purpose of this study was to determine if the use of a laser ablation coating removal (LACR) system would provide the Virginia Department of Transportation (VDOT) with an acceptable new alternative for removing existing coatings. In this study, the LACR process was documented in the laboratory and in the field to determine the feasibility of implementing LACR for VDOT bridges. All LACR work was performed on actual structural steel features from Virginia bridges. Industrial hygiene surveys of the LACR process were used to determine the environmental and worker safety of LACR. Laboratory material analysis of samples evaluated the effects on the properties of steel bridge components.

This work led to the following conclusions.

- LACR effectively removes the coatings investigated, including lead-based coatings. Although microscopic investigation revealed that small coating particles remained on the surface after cleaning (which were not visible to the naked eye), this did not appear to affect subsequent coating adhesion adversely.

- The coating adhesion of LACR surfaces, tested by two independent laboratories, is acceptable.

- LACR does not detrimentally affect the mechanical properties of the ASTM A36 structural steel examined in this study. The tensile yield strength, ultimate tensile strength, ductility, and fatigue strength were on parity with expected values.

- The industrial hygiene study results showed that the engineering controls associated with the LACR system maintained potential exposures to hazardous air pollutants for the laser operator well below the current Occupational Safety and Health Administration's permissible exposure limit and action limit for each constituent sampled within a worker's breathing zone and adjacent work area. This could provide a potential cost benefit, since LACR does not require the type of containment that traditional grit-blasting approaches require.

- Similar to traditional coating removal technologies, the waste generated by LACR was classified as a regulatory hazardous waste; appropriate personal protective equipment must be worn during management of the waste material and filters.

- In the field, the LACR system was effective on bridge beam ends and bulk heads in open spaces but was more problematic in tight spaces where the geometry limited access to the coated surface. The team did observe, but were unable to test in detail, other LACR systems that were smaller, lighter weight, and more powerful.

- LACR can be employed as a lead-based coating removal technique in preparation for other manufacturing processes, such as cutting or welding routinely performed by VDOT. Such applications would not necessarily require high productivity rates or access to tight spaces.

TABLE OF CONTENTS

FINAL REPORT

INNOVATIVE COATING REMOVAL TECHNIQUES FOR COATED BRIDGE STEEL

James M. Fitz-Gerald, Ph.D.
Professor of Materials Science and Engineering, University of Virginia

Sean R. Agnew, Ph.D.
Professor of Materials Science and Engineering, University of Virginia

William Moffat
Graduate Student, University of Virginia

Stephen R. Sharp, Ph.D., P.E.
Senior Research Scientist, Virginia Transportation Research Council

James S. Gillespie
Senior Research Scientist, Virginia Transportation Research Council

Donald R. Becker
Corrosion and Coatings Program Manager, Turner-Fairbank Highway Research Center

Rongtang Liu, Ph.D., P.E.
Engineering Lab Manager, SES Group and Associates

Arthur Runion
Lab Research Assistant, SES Group and Associates

INTRODUCTION

One of the most common methods of preventing corrosion of steel bridge components is to employ polymeric coatings. This is an effective corrosion mitigation technique. However, with time, coatings require maintenance in order to continue to protect effectively the underlying steel, as weathering and exposure can slowly deteriorate these coating systems and leave the steel vulnerable to corrosion. This can especially be seen near the ends of some bridge beams where excessive corrosion damage has occurred because of leaking deck joints, resulting in frequent salt exposure.

Determining the optimal method for maintaining the coating system and protecting the structural steel can be complex and costly. It involves ensuring that the surface is prepared properly and determining that the coating will adhere to the substrate, which is key for mitigating corrosion damage. In addition, coating work in the field must comply with worker health and safety regulations and ensure compliance with environmental requirements through the proper containment of all materials.

The Virginia Department of Transportation (VDOT) spends approximately $160 million every year on bridge maintenance throughout the state, with bridge coating maintenance accounting for approximately 10% of this annual cost.[1] These costs include mobilization, traffic control, worker health and safety, environmental protection, surface preparation, containment, re-coating, and waste disposal. Recently, laser ablation coating removal (LACR) has gained in popularity and use as a viable alternative to conventional coating removal methods such as abrasive blasting, chemical stripping, or power tool cleaning because of its advantages, including smaller amounts of waste generation and potential for selective coating removal.

Laser ablation, which is sometimes referred to as laser cleaning, uses high-energy light pulses that are directed at a target to eject the surface layers of material. Applications range from art and sculpture cleaning and refurbishing,[2-8] paint and graffiti removal,[9] nuclear decontamination,[10] and rust removal[11-13] to coating removal on aerospace[14] and marine structures.[15-20] LACR can effectively remove coatings from steel substrates. Laser ablation has found uses for cleaning building facades, exteriors, and even sculptures and ornaments. The Philadelphia City Hall,[20] U.S. Capitol Building,[21] and Canadian Parliament building[22] are examples of prominent landmarks that have been successfully cleaned using LACR technology.

PURPOSE AND SCOPE

The purpose of this study was to evaluate the effectiveness of LACR for removing existing coatings from bridge components. The two main aspects of interest to VDOT were worker health and environmental safety and the effects of LACR on the underlying substrate. The two main objectives of the study were (1) to determine whether VDOT could implement LACR technology cost-effectively in coating removal operations on bridges, and (2) to identify any additional coating removal techniques that VDOT should evaluate.

To achieve the first objective, the University of Virginia (UVa), the Turner-Fairbank Highway Research Center (TFHRC), VDOT, and the Virginia Transportation Research Council (VTRC) evaluated the response of coated steel elements to LACR, which included comparisons to traditional sand-blasted surfaces. The study was divided into a series of phases designed to test the LACR process in both controlled conditions (laboratory settings) and realistic, on-site bridge or outdoor locations (field settings). Phases 1, 3, and 5 were performed in laboratory settings; Phases 2 and 4 were performed in field settings. During Phases 1, 2, and 4, environmental compliance and industrial hygiene surveys were conducted to determine whether the engineering controls associated with LACR are protective for both the operator and the environment. VTRC, VDOT, and UVa worked together to perform Phases 1 through 4; samples from Phase 1 and coating materials from VDOT were sent to TFHRC for evaluation by the Corrosion and Coatings Lab during Phase 5, the final phase of this study.

To achieve the second objective, new coating removal technologies considered environmentally safe and field ready were pursued. These technologies were identified through electronic searches via the internet and follow-up discussions with vendors.

METHODS

Overview of Evaluation of LACR on Coated Bridge Steel

To achieve the study objectives, the study was divided into five phases:

1. *The environmental and industrial hygiene (IH) requirements in Phase 1 were used to establish the viability of using LACR by VDOT.* Each subsequent phase was used to address questions and develop LACR further as a method for removing coatings from VDOT structures. Phase 1 consisted of using LACR on coated I-beam sections made of structural steel fabricated in accordance with ASTM A36, Standard Specification for Carbon Structural Steel (hereinafter "A36 steel"), removed from a decommissioned bridge structure in VDOT's Lynchburg District. Samples prepared using a traditional method, grit blasting, were also processed. Both the grit blasting and laser ablation operations took place at the facility of the LACR representative. The operation was documented and recorded, and environmental and IH data were collected.

2. *Phase 2 included an on-site field demonstration where LACR was tested on an in-service bridge structure in VDOT's Lynchburg District.* An IH assessment was conducted during this operation.

3. *In Phase 3, sections of a bridge bearing were transported to the facility of the LACR representative, and another LACR test was performed.* The purpose of this test was to determine whether the LACR was capable of cleaning the surfaces of recessed areas of the bridge beam, which were difficult to reach in the field testing performed in Phase 2.

4. *Phase 4 explored LACR as a lead-based coating removal method.* The purpose of Phase 4 was to determine the effectiveness of LACR in removing lead-based coatings from steel substrates to provide a lead-free surface for further torch cutting of metal samples, a routine task performed by VDOT. Because of the direct high heat and lack of a vacuum system, torch cutting and other methods of hot metal cutting and shaping can cause large amounts of heavy metal fumes such as lead fume to be generated.

5. *Phase 5 was performed at TFHRC and included the evaluation of steel samples from Phase 1.* In Phase 5, TFHRC coated the Phase 1 panels using coatings provided by VDOT. These coating materials included two Sherwin Williams products, an epoxy primer (Steel Spec Epoxy Primer) and a flake filled epoxy (Macropoxy 646 FF), and two Carboline products, phenalkamine epoxy (Carbogard 690) and epoxy mastic (Carbomastic 15), which were recommended for applications with a minimal surface preparation.

In addition to the physical LACR demonstrations and material testing and characterization, a literature review was conducted. The literature review focused on identifying other novel coating removal techniques that might benefit VDOT.

LACR Phase 1: Laboratory Demonstration

Phase 1 consisted of sample generation and the initial test to laser clean bridge components. Several bridge I-beams were removed by VDOT from the bridge on Route 685 (Telegraph Road) over Stinking River in Pittsylvania County, VDOT Structure No. 6096 (Figure 1); sectioned into 1-ft or 5-ft sections; and transported to the facility of the LACR representative for the LACR demonstration. Along with the documentation and observations made of the LACR process, an IH survey was conducted to monitor and report on the worker health and safety and environmental protection of the process. Phase I took place in an indoor office setting, further demonstrating the cleanness of the process because of the vacuum and filtration system on the laser.

Personal and area samples were collected during the LACR demonstration to evaluate the concentrations of various heavy metals and volatile organic compounds (VOCs) in the work area and associated equipment.

Figure 1. Bridge From Which the 20 I-Beam Samples Were Taken

The coating removal was performed using an Adapt Laser Systems Model CL1000QNd:YAG (1000W) system operating at a fundamental wavelength of 1064 nm and delivering 1 kW of average power. As each I-beam section was cleaned, the process in addition to the IH analysis was documented and recorded. Figure 2 shows the laser unit being used to clean a sample and a close-up of the laser beam surface interaction. It should be noted that the visible light at the end of the optic head is not the laser light itself (which is invisible to the human eye because of its infrared wavelength) but is actually plasma generated by the laser heat and ablation of the surface coatings. The laser settings during LACR were recorded and are provided in Table 1.

(a) (b) (c)

Figure 2. Laser Ablation System and Operation: (a) 1000W system; (b) operation of the laser; (c) close-up of the laser ablation process on one of the I-beams

Table 1. Laser Setting for Each Pass During Phase 1

Sample	Laser Intensity	No. of Passes		
		H	M	L
1A	High (24 KHz), Medium (35 KHz), and Low Intensity (40 KHz)	2	2	2
2A	High (24 KHz), Medium (35 KHz), and Low Intensity (40 KHz)	2	2	2
3	High Intensity (24 KHz)	6		
5	High Intensity (24 KHz)	6		
8	Low Intensity (40 KHz)			6
10	High Intensity (24 KHz)	6		
11	Low Intensity (40 KHz), side flanges are high (24 KHz)	4		6
12	High Intensity (24 KHz)	6		
13	High Intensity (24 KHz)	6		
14	High Intensity (24 KHz)	6		
18	Sand Blasted	N/A	N/A	N/A
19	High Intensity (24 KHz)	6		
L1-L40 †	30 KHz	N/A		

H = High (24 KHz); M = Medium (35 KHz); L = Low Intensity (40 KHz).
† 5-ft long beam rather than 1-ft long beams.

Preparation of Metallurgical Samples for Analysis

The I-beams cleaned in Phase 1 were used for metallurgical analysis and for samples later used in tensile and fatigue tests. For metallurgical testing, the flanges of the beams were removed using a cutting torch; a band saw was subsequently used to cut out roughly 1 in x 1 in

pieces for analysis (Figure 3). The samples were cut in accordance with ASTM E8 from the middle of the I-beam web to avoid any metallurgical effects of thermal damage from torch cutting heat applied to the sides. One of the sides of the dog-bone specimens was then surface-ground to a smooth finish. Sharp edges were also rounded using the same surface grinding tool.

Metallurgical samples were polished using conventional polishing techniques with up to 1200 grit size polishing paper and then with 3 μm, 1 μm, and colloidal polishing solution. Samples were etched using a 2% Nital etchant (2% nitric acid, 98% ethanol v/v). Metallographic analysis was performed for all three processing conditions, including base, laser-cleaned, and grit-blasted material. Both planar analysis and cross-sectional analysis of the roughly 1 in x 1 in sections of base, grit-blasted, and laser-cleaned material were conducted by optical microscopy, using the Hirox optical microscope (Model KH-7700) and the scanning electron microscope (SEM) Models FEI Quanta 200 and FEI Quanta 650. Painted samples were sputter coated using an Au/Pd target in a Technics Sputter Coater. In addition to microscopy, composition was determined in samples of all three processing conditions using energy dispersive spectroscopy (EDS). EDS spot, line, and area mapping modes were used to measure the elemental composition of cross sections, surface layers, and top planar surfaces for the three processing conditions.

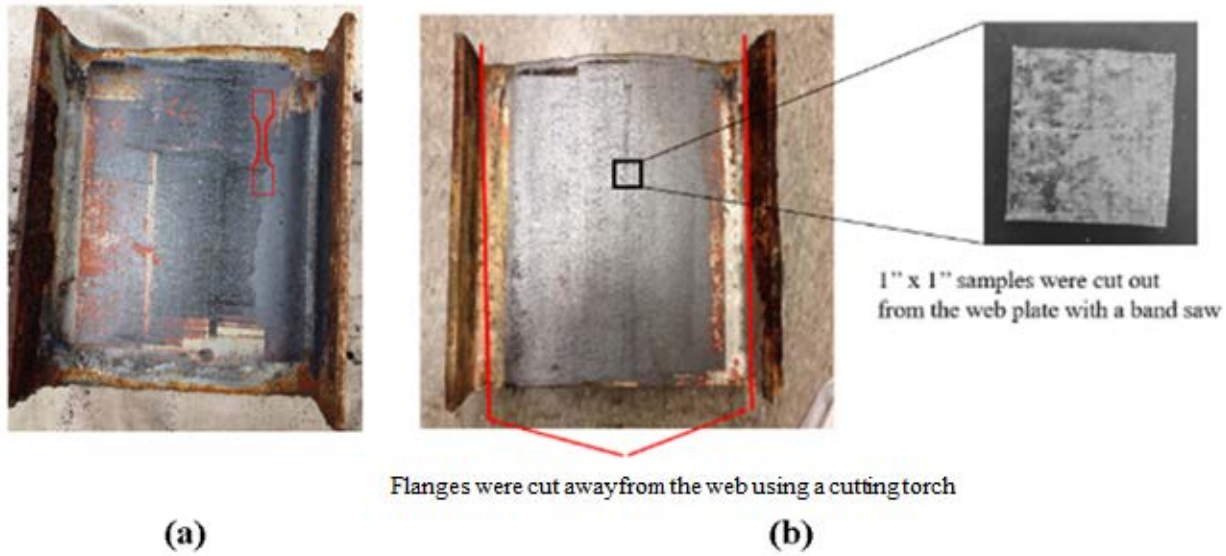

Figure 3. Sample Preparation: (a) mechanical test samples; (b) samples for metallurgical analysis

Coating Adhesion Testing

After the beams in Phase 1 were laser ablated, samples were recoated with standard epoxy mastic paint for coating adhesion testing using the pneumatic adhesion tensile testing instrument (PATTI) device. The PATTI device is used to test the coating adhesion of paint to the underlying substrate and conforms to the requirements of ASTM D4541 and ASTM D7234 for coating adhesion testing. Figure 4 shows the surface of a laser-cleaned flange and the repainted surface with the PATTI pull-stubs attached. In addition, coating adhesion testing was performed on steel samples from Phase 1 using either LACR or grit blasting in Phase 5, as discussed later.

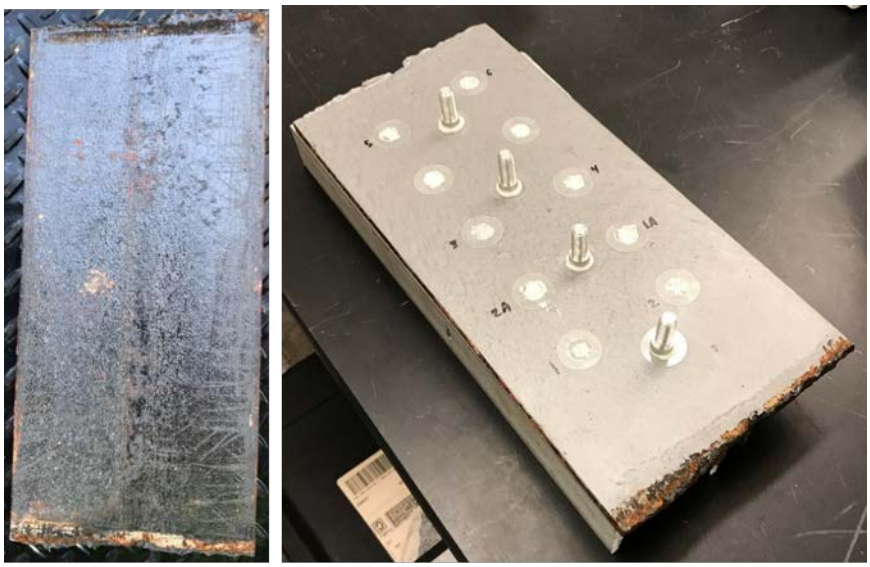

(a) (b)

Figure 4. LACR-Cleaned I-Beam Flange: (a) before and (b) after repainting with PATTI stubs. LACR = laser ablation coating removal; PATTI = pneumatic adhesion tensile testing instrument.

Mechanical Testing

To determine the effects of laser ablation on the mechanical properties of the underlying metal, tensile, fatigue, and hardness tests were performed. Hardness tests were performed on cross sections for each processing condition. Vickers hardness measurements were taken as a function of depth from the surface of the metal down into the middle of the cross sections. A standard diamond-tipped Vickers hardness indenter was used with a mass of 0.5 kg and an indentation time of 15 seconds. Tensile testing included pulling dog bones of the base metal, grit-blasted metal, and laser-cleaned samples. Tensile tests were performed on a MTS Systems Corporation (MTS) Series 793 servo-hydraulic universal testing machine and used a laser extensometer to measure the initial gauge length and the gauge length elongation during the test in accordance with ASTM E8. Fatigue testing was performed on the same Instron machine frame in a pull-pull configuration, so that the dog bones were always under tensile stress, with a fatigue ratio, R, of 0.1 at 10 Hz in accordance with ASTM E466. Samples that did not fail before 5 million cycles were considered run-out tests and were stopped upon reaching this number of cycles. In addition, in Phase 5, mechanical testing was performed at TFHRC on steel samples from Phase 1, as discussed later.

LACR Phase 2: Field Demonstration

Phase 2 consisted of an on-site demonstration of the feasibility of using the LACR system on a VDOT bridge structure. The laser testing was performed on the Route 695 Bridge in Prince Edward County, Virginia, near Farmville. Figure 5 shows the underside of the bridge where the LACR was attempted. The laser generator, filtration unit, electrical generator, and associated equipment were housed and operated from a trailer that was parked on the side of the road below the bridge, and a boom lift was used to bring the laser operator and laser optic within working

distance of the bridge components (Figure 5). To operate the LACR system, a generator capable of providing 480 V was required.

In order to supplement the on-site LACR documentation and observation, the VDOT industrial hygienist monitored the potential occupational exposures and environmental protection associated with the process. During the demonstration, a tarp was hung behind the laser operator in the lift to ensure that no reflected laser light was allowed to escape to the surrounding area, and routine laser safety protocols, such as wearing laser safety glasses, were in place.

Personal and area samples were collected during the LACR demonstration to evaluate the concentrations of various heavy metals and VOCs in the work area and associated equipment.

Figure 5. On-site Demonstration of LACR: (a) underside of Route 695 Bridge in Farmville, Virginia, where the on-site LACR testing took place; (b) boom lift used to elevate the operator to the cleaning area. LACR = laser ablation coating removal.

LACR Phase 3: Cleaning Tight Geometry Area Demonstration

Phase 3 was conducted to determine the capability of the 500W Adapt Laser (500W) System to clean minimally accessible areas such as bridge beam ends and bearings effectively. For this demonstration, on November 9, 2017, a bridge bearing provided by VDOT was transported to the facility of the LACR representative in Chesapeake, Virginia, to perform the laser ablation. A bridge bearing was chosen because of the recessed areas that could be used in this Phase 3 test. The bearing component selected for LACR is shown in Figure 6.

In order to evaluate the ability for the laser to clean tighter areas, the 500W system was used with the CleanCUBE H15 head, which consists of a laser optic head with a light aperture that is 90 degrees to the incoming optic cable line, allowing for a more maneuverable optic that also takes up less space (Figure 7). The targeted area for the laser test was one of the recessed areas underneath the bearing pin because it was the toughest part of the bearing to access with the laser. After surface scale and dirt were removed by hand with a metal scraper and wire brush, the first attempt at laser ablation used the 500 Watt laser and CleanCUBE H15 optic.

Figure 6. Bridge Bearing Component Used in Phase 3

Figure 7. CleanCUBE H15 Optic Head Used With the 500 Watt Laser. The optical cable (green) enters the head from the laser power supply. The cleaning lens is on the left in both images.

Although a hand-held version of the CleanCUBE head has been developed, only a robot-mountable version was available, which hindered optimal use of the laser. For example, the laser had to be triggered by another operator at the laser generator unit. In addition, the CleanCUBE head system was not equipped with a vacuum system, so a handheld external vacuum nozzle unit was used to remove fumes, as shown in Figure 8. This allowed for improved access to the surfaces, but the head was still bulky, heavy, and without a built-in vacuum system. During this demonstration, an IH survey was not conducted, so the effectiveness of the external vacuum system was not evaluated. Although it is presumably less effective than an integrated vacuum nozzle when used with the optic head, which ensures that the ablated material follows the precise position of the laser, additional evaluation is warranted to determine the effectiveness of the external vacuum engineering controls.

Various apertures with different corresponding laser focal lengths can be used with the 500W system, and different combinations of lenses and laser parameters were tested until an optimal setup was found. The first laser setup used the 150 mm lens, which has a focal length of 6 in. This was later replaced with the 250 mm lens, which increased the focal length to 10 in. Various laser parameters such as pulse frequency and scan width were adjusted until optimal settings were found. After the settings on the laser were adjusted, a test scan was performed on a sample piece of scrap metal to determine the characteristics of the beam before the laser was used on the bearing.

Figure 8. Images of Right-Angle CleanCUBE Head Geometry Processing in Tight Geometric Areas

Table 2 shows the different laser parameters tested in sequential order, ending with the perceived best configuration. The specific laser parameters can, and likely will, vary depending on the specific area and geometry of the part to be laser ablated and the nature of the coating being removed.

Table 2. Various Laser Parameters Investigated During Testing

Test No.	Aperture	Pulse Frequency	Scan Width
1	150 mm	22 KHz	75%
2	250 mm	18 KHz	75%
3	250 mm	18 KHz	50%
4	250 mm	18 KHz	30%

LACR Phase 4: Testing for Lead Abatement

With LACR demonstrating favorable performance during the earlier phases, VDOT conducted an occupational hazard study to characterize the effectiveness and safety of lead removal by LACR as a technique to prepare girders for subsequent hot work. VDOT conducted IH and air sampling on location, which also included lead wipes testing. Electron microscopy and EDS were then performed on hot work samples at UVa. Some of the findings are reported here; a full report of this portion of the study is available elsewhere.[23]

The first stage of Phase 4 took place on July 30, 2018, at the facility of the LACR representative in Chesapeake, Virginia. In this stage, bulk samples, wipe samples, XRF readings, and air samples for lead, hexavalent chromium, and polychlorinated biphenyls were collected while two employees used a 1000W system to remove 55 linear inches of coating from beams provided by VDOT. Following this initial stage, personal and area IH samples for lead were collected while a VDOT employee completed oxyacetylene torch cutting, plasma torch cutting, and grinding on the two beams on August 1, 2018, at VDOT's Hampton Roads District Office.

After VDOT conducted the laser ablation and hot cutting of the beam, the IH survey, and the contracted lead testing, cut sections of the I-beams were transported to UVa for further

surface characterization. After smaller (roughly 1 in x 1 in) metal samples were cut out from the I-beams, the surfaces were studied using the SEM and XRF (X-ray fluorescence), with the primary goal of measuring the remaining amount of lead on the surface.

LACR Phase 5: TFHRC Steel Surface and Coating Evaluation

For the Phase 5 evaluation, beam sections cleaned during Phase 1 by LACR or grit blasting were transported to TFHRC along with four different coating materials. The first set of steel samples included two 5-ft-long I-beam sections, shown in Figure 9. The web of one beam was grit blasted, and the web of the other one was laser ablated with a laser intensity of 30 KHz. The second set consisted of twelve 1-ft-long sections of I-beam, of which one (ID 18) was grit blasted and the rest were laser ablated with various intensities, as shown in Table 1.

The web of the beams was sawn into 3 in x 5 in panels. An identification number was stamped on each panel so that the laser-ablated and grit-blasted panels could be tracked.

The coating materials provided by VDOT to TFHRC included two Sherwin Williams products: an epoxy primer (Steel Spec Epoxy Primer) and a flake filled epoxy (Macropoxy 646 FF), and two Carboline products, phenalkamine epoxy (Carbogard 690) and epoxy mastic (Carbomastic 15). These materials were recommended for applications with a minimal surface preparation.

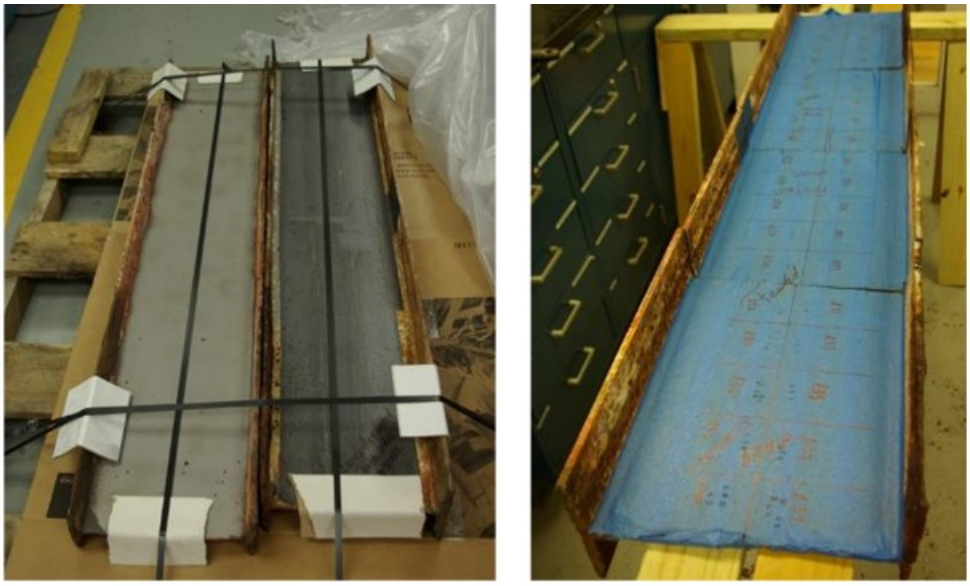

(a) (b)

Figure 9. Steel Beams: (a) as received; (b) ready to be sawn into 3 in x 5 in panels

Upon receipt of the test materials, the following tests were performed by TFHRC to evaluate the steel surface preparation for corrosion and coating performance compared to the grit-blast coating removal method:

- surface profile (ASTM D4417)
- tensile strength of the steel (ASTM E8/E8M)
- adhesion strength of the coating systems (ASTM D4541)
- soluble salts on the surface (SSPC Technology Guide 15)
- electrochemical tests (corrosion potential, instant corrosion rate, and polarization resistance)
- coating performance after cyclic exposure tests.

TFHRC applied the coatings to the Phase 1 samples in accordance with the instructions of the coating material manufacturers. Tests were performed on the coated panels to evaluate the performance of the coating systems as the panels went through cyclic exposure conditions. These performance-related factors included surface defects, rust creepage, and changes in physical and chemical properties such as color, gloss, and adhesion. The following tests were performed:

- dry film thickness (DFT) (ASTM D7091 or SSPC-PA2)
- gloss loss (ASTM D5230)
- color change (ASTM D2244)
- adhesion (ASTM D4541)
- average rust creepage (ASTM D7087).

Evaluation of Uncoated Phase 1 Steel Samples

Yield and Ultimate Tensile Strength Testing

Using material left over from the beams that were sectioned for the paint panel tests, tensile test specimens were made for yield and tensile pull tests. Originally, two different beams that had the coating removed using grit blasted or LACR were delivered to TFHRC. Specimens from both beams were used to make the tensile test samples.

Testing was conducted in accordance with ASTM E8-16a[24] using a specimen that was the standard ½-in width along the gauge length. The dimensions of the specimens as measured are listed in Table 3.

Table 3. Specimen Numbering and Measured Dimensions

ID	Reduced Section Length, in	Width, in				Thickness, in				Calculated Area, in^2
		Top	Middle	Bottom	Average	Top	Middle	Bottom	Average	
1	3.500	0.490	0.490	0.490	0.490	0.250	0.250	0.250	0.250	0.123
2	3.500	0.500	0.500	0.500	0.500	0.255	0.255	0.255	0.255	0.128
3	3.500	0.490	0.490	0.490	0.490	0.255	0.255	0.255	0.255	0.125
4	3.500	0.490	0.490	0.490	0.490	0.260	0.260	0.260	0.260	0.127
5	3.500	0.490	0.490	0.490	0.490	0.250	0.250	0.250	0.250	0.123
6	3.500	0.490	0.490	0.490	0.490	0.255	0.255	0.255	0.255	0.125
7	3.500	0.490	0.490	0.490	0.490	0.250	0.250	0.250	0.250	0.123
8	3.500	0.490	0.490	0.490	0.490	0.250	0.250	0.250	0.250	0.123
9	3.500	0.490	0.490	0.490	0.490	0.255	0.255	0.255	0.255	0.125
10	3.500	0.495	0.495	0.495	0.495	0.255	0.255	0.255	0.255	0.126
11	3.500	0.500	0.500	0.500	0.500	0.255	0.255	0.255	0.255	0.128

Tests were run on a 25 kip MTS servo-hydraulic test frame, using hydraulic wedge grips. A calibrated MTS strain extensometer was used to span a 1-in gauge section of the test specimens. The tests were run under automated control, using MTS's TestSuite software. Load and strain rates were set in accordance with ASTM E8.

Steel Composition

Chemical analysis was performed on both beams using a Leco spark spectrometer. As no identifying marks were on the beam flanges, the beams were identified as wide flange vs. narrow flange (there was one of each type for material selection).

Two samples were cut into 1.0 x 1.0 x 0.50 in cubes, one from each beam. Those specimens, after machining, were sanded with progressively finer grit papers that were aluminum oxide-based, ending with a very fine crocus cloth paper (also aluminum-based.) Carbide-based paper was not used so as not to leave any residue of carbides on the sample that would be detected by the spectrometer. After sanding, the samples were placed in the spectrometer, where they were held in place by a vacuum at the measurement head. The chemical composition was then determined for each sample.

Surface Profile Evaluation

The grit-blasted and laser-cleaned surfaces were observed under an optical microscope. The surface profile of the steel panels was measured with a surface profile gauge in accordance with ASTM D4417, Standard Test Methods for Field Measurement of Surface Profile of Blast Cleaned Steel, Method B: Surface Profile Depth Gage.[25]

Soluble Salt Analysis on Steel Surface

Extraction of soluble salts from the steel surface was performed in accordance with the SSPC Technology Guide 15, *Field Methods for Extraction and Analysis of Soluble Salts on Steel and Other Nonporous Substrates*.[26] Latex cells were used for surface sampling. The latex patch has a self-adhesive pad with an extraction area of 12.5 cm^2. The CHLOR*RID specialty

extraction solution was used for more effective extraction. The proprietary extraction solution is claimed to "enhance retrieval rates."[27]

The extracted solution was filtered using a syringe filter with a pore size of 0.2 µm. The syringe, filter, and sample vial were washed with deionized water before the filtration process. The final liquid sample was clean and transparent. The concentrations of anions in the aqueous samples were then determined with ion chromatography.

Electrochemical Corrosion Testing

Electrochemical tests (corrosion potential, instant corrosion rate, and polarization resistance) were performed with a paint test cell, as shown in Figures 10 and 11. A paint test cell with an O-ring on its base was clamped to the steel surface with magnets, keeping the apparatus watertight. Deionized water (50 mL) was poured into the glass tube and stirred with a glass rod. The reference electrode was a saturated silver/silver chloride electrode (SSC). The counter electrode was a graphite rod. A potentiostat (Gamry Reference 600+) was used to measure the corrosion potential and the linear polarization resistance. The corrosion penetration rate, in mils per year, was based on the linear polarization resistance measurement. All measurements were carried out at room temperature (75 °F).

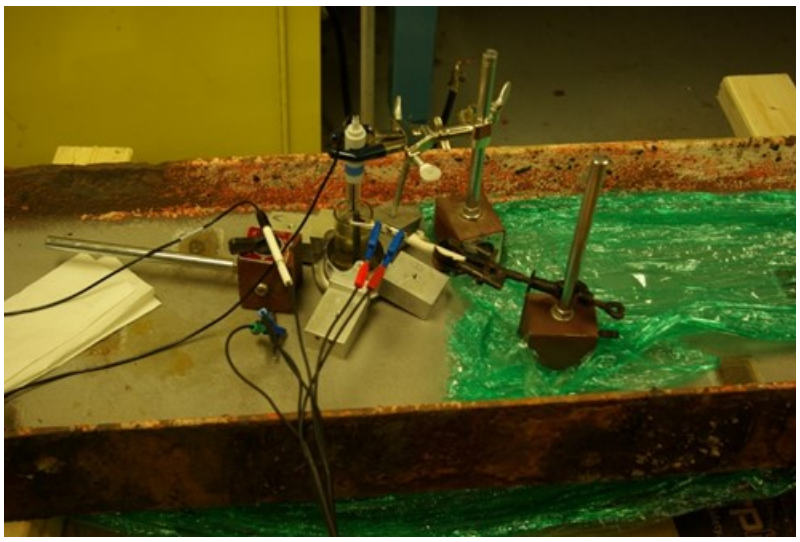

Figure 10. Electrochemical Test on 5-Ft-Long Beam

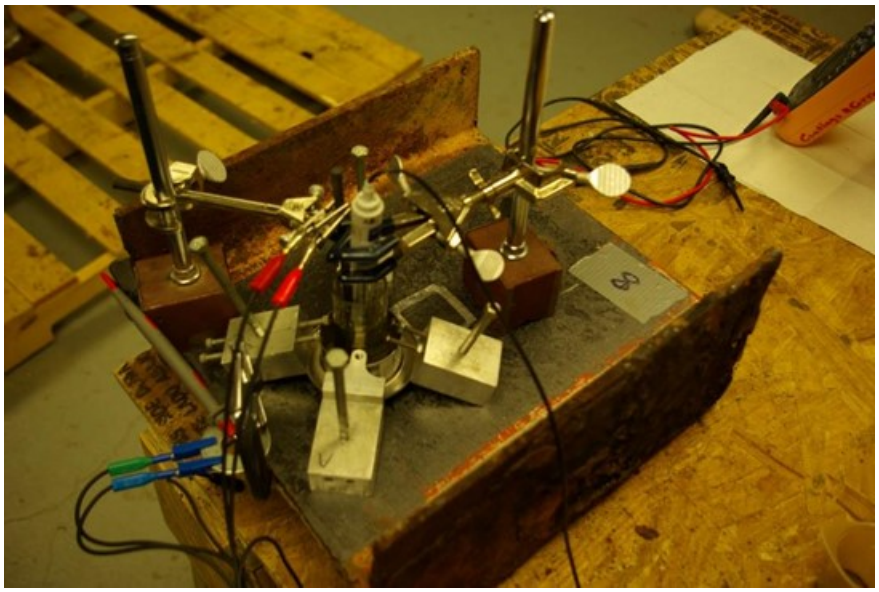

Figure 11. Electrochemical Test on 1-Ft-Long Beam

Coating Assessment

The steel panels were painted with a roller per the manufacturer's instructions. DFT was measured with an electronic gauge in accordance with SSPC-PA2, Measurement of Dry Coating Thickness with Magnetic Gauges,[28] and ASTM D7091.[29] Three DFT spot readings were obtained from each panel.

Cyclic Exposure of Coated Steel Panels

The coating systems were evaluated using accelerated laboratory testing (ALT). The operating procedures for ALT are based on ASTM D5894, Standard Practice for Cyclic Salt/Fog/UV Exposure of Painted Metal (alternating exposures in a fog/dry cabinet [Figure 12] and a UV/condensation cabinet).[30] The salt concentration for the salt/fog was modified to increase its corrosivity. The panels went through 14 ALT cycles and were evaluated after each cycle for color, gloss and rust creepage. Each cycle lasted 360 hours with the conditions and durations provided in Table 4.

The initial conditions of the panels were determined before their exposure to ALT. The following tests were performed after every 360-hour cycle exposure in the ALT chamber:

- rust creepage
- color change
- gloss loss.

After 14 cycles of ALT exposure, the panels were photographed.

Figure 12. Coated Panels in Salt/Fog Chamber of Test Cabinet

Table 4. 360-Hour Cycle: ALT Conditions and Durations Used

Step	Condition	Duration
Freezing	Temperature: -10 °F	24 hr
UV/condensation	4-hr UV/4-hr condensation cycle UV: 340 nm irradiance Temperature: 140 °F Condensation temperature: 104 °F	168 hr
Prohesion	1-hr wet / 1-hr dry cycle. Wet cycle: Fog is introduced at ambient temperature. A mixture of 0.35% ammonium sulfate and 0.5% sodium chloride is used. Dry cycle: Air is preheated to 95 °F and then purged to the test chamber.	168 hr

ALT = accelerated laboratory testing.

Effect of Surface Treatment on Coating Adhesion Strength

Adhesion strength testing was performed before and after cyclic exposure. The adhesion strength of the coating systems was determined using the pull-off adhesion tester in accordance with ASTM D4541-09, Standard Test Method for Pull-Off Strength of Coatings Using Portable Adhesion Testers.[31] A loading fixture, commonly known as a dolly or stub, was affixed to the panel surface by an adhesive. A load provided by the adhesion tester was increasingly applied to the dolly until it was pulled off. The force required to pull off the dolly yielded the tensile strength (psi or MPa). Failure occurs along the weakest plane(s) within the testing system comprised of the dolly, adhesive, individual layers of the coating system, and substrate.

The surfaces of the coated test panels and the base of the dollies were cleaned with alcohol and lightly roughened with sandpaper. The dollies were glued to the test panel surface using a high-strength epoxy adhesive. The adhesion strength was measured by the hydraulic method. Three pull-off adhesion tests were performed on each test panel. For every panel, the average adhesion strength of three locations was calculated. If the coefficient of variance of each test panel was more than 20 percent, the test panel and adhesion failure mode were carefully examined to see if the variation was caused by test operation. Repeat tests were performed for quality assurance. If more than 50 percent of a glue failure occurred, the test was repeated. The pull-off strength and failure mode were recorded.

Effect of Surface Treatment on Coating Specular Gloss

Gloss for every coating was measured in accordance with ASTM D5230-08, Standard Test Method for Specular Gloss.[32] Geometry measurements (20 degree and 60 degree) were conducted on the un-scribed panels before and after cyclic exposure. Three gloss readings for each were recorded.

Effect of Surface Treatment on Coating Color

The color of the coatings was measured using a 45-degree / zero-degree colorimeter in accordance with ASTM D2244-09A, Standard Test Method for Calculation of Color Differences from Instrumentally Measured Color Coordinates.[33] This technique is based on the calculation from instrumentally measured color coordinates based on daylight illumination of color tolerances and small color differences (ΔE) between opaque coated panels. The International Commission on Illumination (CIE) lab color system (CIE [L*, a*, b*]) was used for color measurement. L*, a*, and b* represent the three coordinates of the three-dimensional lab color space. These parameters are defined based on the following high and low values they represent to identify colors:

- L* = 0 represents black, and L* = 100 represents diffuse white.
- Positive values of a* indicate green, and negative values indicate magenta.
- Positive values of b* indicate blue, and negative values indicate yellow.
- The asterisk (*) is used to differentiate the CIE (L*, a*, b*) system from the L, a, and b parameters of the original Hunter 1948 color space.

Color readings were measured before and after ALT. Three color readings were obtained from each reading location. Three locations were measured for each panel. The ΔE of the test panels before and after the test was calculated using the following equation:

$$\Delta E = [(\Delta L^*)^2 + (\Delta a^*)^2 + (\Delta b^*)^2]^{1/2}$$

where

$\Delta L^* = L^*_{\text{after test}} - L^*_{\text{before test}}$
$\Delta a^* = a^*_{\text{after test}} - a^*_{\text{before test}}$
$\Delta b^* = b^*_{\text{after test}} - b^*_{\text{before test}}$.

Rust Creepage Testing

Prior to ALT, coated panels were scribed with a sharp blade to create a 50-mm-long groove (Figure 13). The rust creepage at the scribe was measured in general accordance with ASTM D7087-05A, Standard Test Method for an Imaging Technique to Measure Rust Creepage at Scribe on Coated Test Panels Subjected to Corrosive Environments.[34]

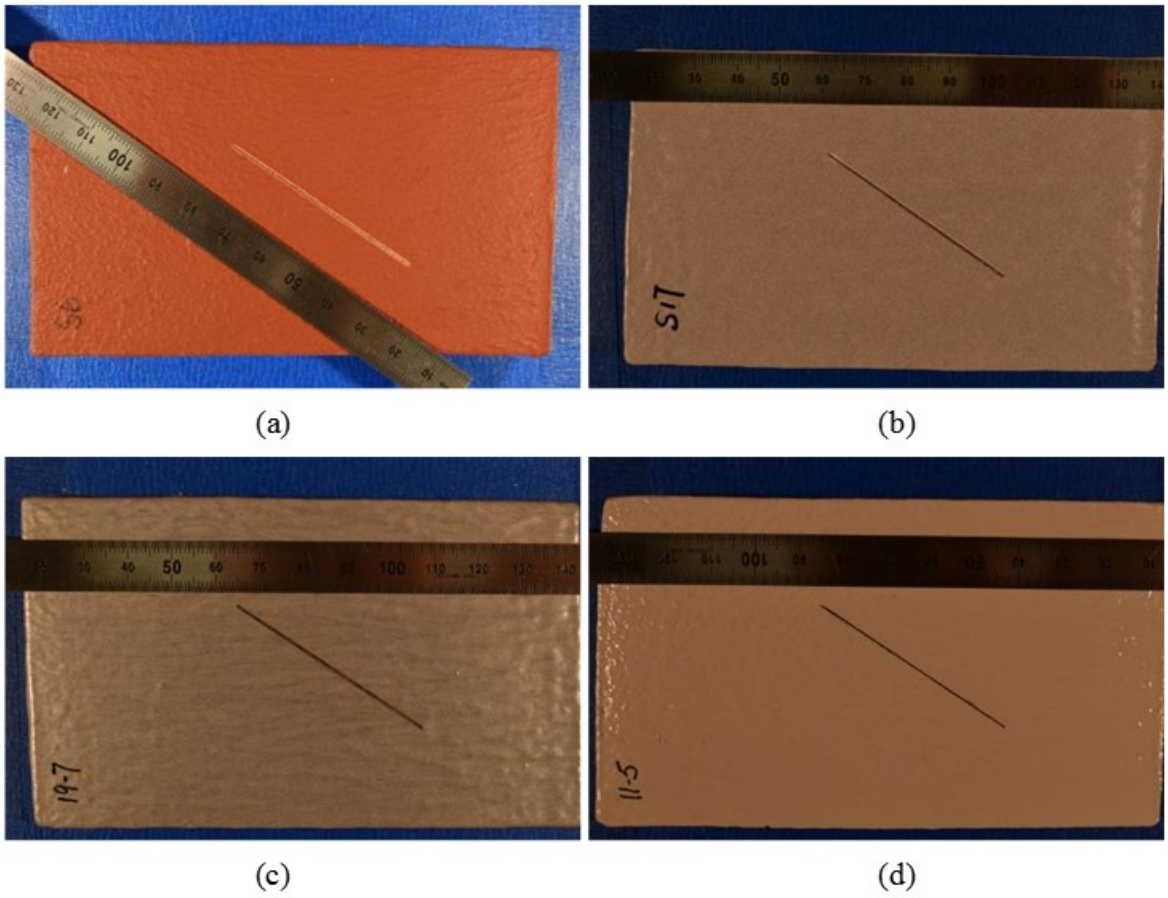

Figure 13. Scribed Panels for Coatings Tested: (a) Steel Spec Epoxy Primer; (b) flake filled epoxy; (c) epoxy mastic; (d) phenalkamine epoxy

The rust creepage area from the scribe line on the coating panel was traced using a fine pencil or marker. The tracing line was photographed and analyzed using imaging software to obtain the creepage areas and creepage distances.

ImageJ was the software package used to measure the rust creepage. The following steps were performed to do this:

1. Open the file.

2. Magnify the image (using Magnifying Glass).

3. Write the panel ID, test cycle, dates, etc. Use Text Tool to write, and then click EDIT>DRAW to etch the text on the image.

4. Set the scale: Analyze>Set Scale.

5. Mark the length. Draw a 40-mm straight line parallel to the rusted scribe line as shown in Figure 14. Place the marking line outside the rust creepage area. Position the line at the middle of the scribe line.

6. Sketch the Creepage Outline as shown in Figure 15. For better results, use fine lines—size 1. Use Polygon Selections.

7. Measure the area of the polygon (ANALYZE>MEASURE).

8. Label the area (ANALYZE>LABEL).

9. Write the value of the area, in mm^2, with TEXT TOOL, and then click EDIT>DRAW.

10. Save the new file.

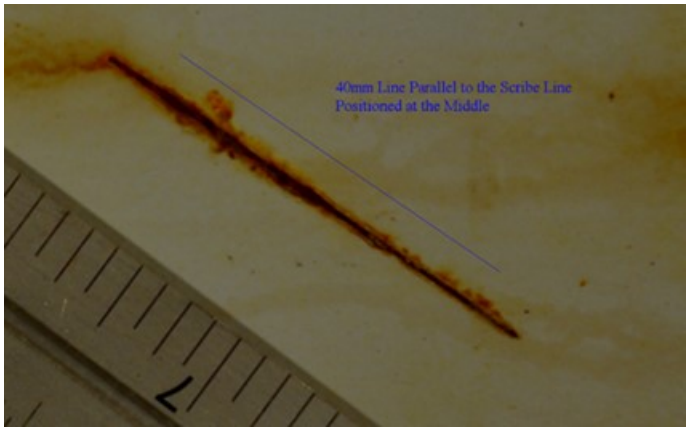

Figure 14. Marking Scribe Length in ImageJ

Figure 15. Sketching Rust Creepage Outline on Image

Industrial Hygiene and Environmental Evaluation

For the IH and environmental work during Phases 1 and 2, personal and area samples were collected during the laser coating removal demonstration to evaluate the concentrations of various heavy metals and VOCs in the work area and associated equipment.

This survey was conducted in compliance with the Occupational Safety and Health Administration's (OSHA) General Industry Standard: Subpart Z, Toxic and Hazardous

Substances. During Phases 1 and 2, the survey documented personal and area concentrations of a 31-profile scan of VOCs using an Assay 566 badge and included a nine-metal profile sampling (Cd, Cr, Co, Cu, Fe, Pb, Mn, Ni, and Zn) in accordance with National Institute for Occupational Safety and Health (NIOSH) Method 7300 to capture contaminants emitted in the air associated with the simulated bridge coating removal operation. The VOCs in the Assay 56 badge profile included methyl chloroform;1,1,2- trichlorethane; 1,1-dichloroethane;1,2-dichlorethane; acetone; benzene; chlorobenzene; cumene; cyclohexane; cyclohexanone; cyclohexene; ethyl alcohol; ethylbenzene; isopropyl alcohol; m-dichlorobenzene; methyl ethyl ketone; methyl isobutyl ketone; methyl n-propyl ketone; methylene chloride; n-butyl acetate; n-hexane' n-propyl acetate' 0-dichlorebenzene; para-Dichlorobenzene; pentane; tetrachloroethylene; tetrahydrofuran; toluene; trichloroethylene; and xylene.

During Phase 4, cadmium, PCB, chromium, and hexavalent chromium sampling was performed in the work area. The metals and compound results were compared to OSHA requirements.

Consideration of Additional Techniques for Coating Removal

To identify novel techniques that VDOT should evaluate for coating removal, a search was performed. Technologies that were considered environmentally protective, worker and material safe, and potentially field ready were pursued. This was done by follow-up discussions with vendors.

RESULTS AND DISCUSSION

LACR Phase 1: Laboratory Demonstration

The results gathered in this study ranged from general observations to the characterization of the microstructure of the steel to the results of mechanical and coating adhesion testing. The first results obtained were the general observations made during the Phase 1 cleaning of the I-beam sections at the facility of the LACR representative. During this demonstration, the process of laser coating removal was documented, and this provided a sense of the effectiveness and feasibility of using the laser to remove paint, rust, tar, and dirt from the beams. The bridge from which the samples were taken was built in 1932, and the beams themselves were built circa 1925; as such the I-beam sections showed large amounts of corrosion damage, tar, paint, and debris that had accumulated over the years. Because of the thickness of the rust layers, a metal scraper was used manually to remove flakes of rust before laser ablation began. Figure 16 shows an example of a laser-cleaned area surrounded by the original condition of the surface. In general, three to six passes were required before all the rust, paint, tar, and other detritus were removed. Laser tracks, or streaks, were observed after LACR.

Figure 16. Laser-Cleaned Surface Area and Surrounding I-Beam Surface Area Prior to Cleaning

These were parallel to the scanning laser beam and appeared darker than the surrounding substrate, as shown in Figure 17. The appearance of the tracks varied with the laser parameters used, including scan speed, pulse frequency, and the actual motion of the laser by the operator. In addition to the "darker" and "lighter" colors of these laser tracks, there appeared to be splotchy areas consisting of the darker-colored and lighter-colored areas surrounding these spots.

Figure 17. Photographs of Laser-Cleaned Area: (left) laser "tracks" left behind on surface after laser ablation; (right) higher magnification of region between tracks of random surface pattern of darker- and lighter-colored regions. Surface roughness was characterized parallel and perpendicular to the laser tracks.

Aside from the appearance of the laser-cleaned surface, it was also noted that the red paint was more difficult to remove compared to the other paint coats. With a greater number of laser passes, this red paint could be completely removed; however, it often required more passes with the laser than with the other paint coats needed for "complete" removal. Therefore, a noticeable amount of surface area still contained the red paint layer. Of the 20 1-ft I-beam sections, 18 were laser ablated and 2 were grit blasted on-site at the facility of the LACR representative as a comparative processing condition for further material characterization.

Speed of Operation

As noted previously, the two test beams dated to about 1925. The oldest design manual the authors retrieved was the 1949 American Institute of Steel Construction (AISC) *Steel Construction* manual. One beam appeared to match what is called an "8 x 4" I-beam, each with a depth of 8.00 in, a web thickness 0.441 in, a flange thickness of 0.425 in, and a flange width of 4.171 in. The other beam appeared to be a back-to-back pair of what are called "9 x 2.5" channel beams, each with a depth of 9.00 in, a web thickness of 0.230 in, a flange thickness of 0.413 in, and a flange width of 2.430 in.

The demonstration indicated that the experimental operators were able to work about twice as fast with a roller as they could without a roller. Using a laser head without a roller, the operators removed paint from 55 linear inches on "five sides" (one channel plus the top and bottom surfaces) at the end of each beam in 197 min. As the lateral width of "five sides" would be 20.072 in on the 8 x 4 beam and 23.120 in on the back-to-back 9 x 2.5 beams, the speed of removal would equal 12.059 in^2/min. Using a laser head with a roller, the same operators removed paint from 55 linear inches on "three sides" (one channel) at the end of each beam in 53 min. As the lateral width of "three sides" would be 11.730 in on the 8 x 4 beam and 13.400 in on the back-to-back 9 x 2.5 beams, the speed of removal would equal 26.0783 in^2/min.

A distinctive feature of the laser unit is that the light beam comes into focus at one precise distance: in the case of the unit used in the demonstration, this distance was 6 in from the tip of the head attachment. At the point of focus, the laser is so intense that it heats the coating past the gas phase to the plasma phase. At a longer or shorter distance the beam, out of focus, is only hot enough to set the coating aflame; this effect is spectacular, but it does not allow coating removal at efficient speed (neither is it desirable for environmental containment or IH). The purpose of the roller is to maintain the laser head at a distance from the coating surface equal to the focal length of the laser. The observed difference between operating speed with and without the roller quantifies the speed cost to an operator who has to maintain the proper distance by hand and eye alone.

Industrial Hygiene

A consulting group was used to perform the IH testing during this phase of the study. Figure 18 shows the personal sampling devices worn by the laser operator. Two operators used the system over a time designed to approximate an 8-hour shift, employing the metal profile area collection on their belts and the VOC assay badges clipped to their collars within the breathing zone.

(a) (b)

Figure 18. Personal Industrial Hygiene Sampling Setup: (a) operator wearing VOC collector on his belt with a tube leading to the breathing zone; (b) VOC collector collecting units used for area placement. VOC = volatile organic compounds.

In terms of static operation locations, the first metal profile sample was placed approximately 12 ft away from the work table where the laser removal activities were taking place; the second sample was set approximately 2.5 ft from the filter exhaust point of the laser fume extractor; and the third area sample was placed approximately 20 ft away from the laser, adjacent to the rear wall of the test room.

The air monitoring results indicated that the personal and area concentrations of the 31 selected VOCs and metals were below the OSHA permissible exposure limit (PEL) as an 8-hour time-weighted average during the sampling period. In addition, all of the area and personal samples were below laboratory detection limits for all sample contaminants with the exception of lead, which was detected but was below the action level (AL) (30 µg/m^3) and PEL (50 µg/m^3). The lead 8-hour time-weighted averages were 2.2 µg/m^3 for Operator 1 and 0.95 µg/m^3 for Operator 2. Table 5 summarizes the PEL and AL concentrations for the nine metals that were surveyed and collected in the area and personal samples.

Table 5. OSHA Exposure Limits as an 8-hour time-weighted average

Contaminant	OSHA PEL, µg/m^3	OSHA AL, µg/m^3
Cadmium (1910.1027)	5	2.5
Chromium	1000	N/A
Cobalt	100	N/A
Copper	100 (fume)	N/A
Iron oxide	10000	N/A
Lead (1910.1025)	50 (c)	30
Manganese	5000	N/A
Nickel	1000	N/A
Zinc oxide	5000 (fume)	N/A

OSHA = Occupational Safety and Health Administration; PEL = permissible exposure limit; AL = action level; N/A = not applicable.

Lead (Pb) concentrations in the personal air filters of the two laser operators were measured at <2.8 μg/m^3 and <4.0 μg/m^3. These measurements employed NIOSH Method 7082, which the NIOSH manual says is accurate to ±17.6%. VDOT's Environmental Division provided for comparison a lead measurement from the personal air filter of an operator during a grit-blasting operation: this was 33,800 μg/m^3. This measurement employed NIOSH Method 7300; the NIOSH manual gives no "accuracy" level for Method 7300, but it says that the "Percent RSD" is ±6.12 percent or lower, depending on the filter medium selected for the test. Although samples of sizes N = 2 and N = 1 do not support a proper t-test, the reader will note that in these particular samples the lead concentrations in the personal air of the laser operators were 4 orders of magnitude lower—and many confidence intervals lower—than the lead concentration in the personal air of the grit blaster operator.

Cadmium (Cd) and chromium (Cr) levels in the personal air filters of the two laser operators were measured at <2.8 μg/m^3 and <4.0 μg/m^3 (Cd) and at <5.7 μg/m^3 and <8.0 μg/m^3 (Cr). These measurements likewise used NIOSH Method 7082M. Cadmium and chromium levels in the operator air sample from the grit blasting operation were measured at <20.8 μg/m^3 and 314 μg/m^3, respectively. These measurements likewise used NIOSH Method 7300. Again, the samples did not support a t-test, but the reader will note that in these particular samples the cadmium and chromium concentrations in the personal air of the laser operators were 2.5 to 3 times lower than the concentrations in the personal air of the grit blaster operator.

Environmental Compliance

Toxicity characteristic leaching procedure (TCLP) testing was performed on several components of the LACR system filter after completion of the laser removal process. The TCLP testing was conducted in accordance with U.S. Environmental Protection Agency Methods SW6010C and SW7470A and included Ag, As, Ba, Cd, Cr, Hg, Pb, and Se. The sampling was conducted to determine whether the samples would be considered a regulatory hazardous waste because of the characteristic of toxicity. Characterization sampling was conducted on three different parts of the filter system: TCLP Sample 1 was associated with the activated carbon filter, TCLP Sample 2 with the HEPA filter, and TCLP Sample 3 with the particle debris filter. TCLP Sample 1 showed that all metals were below the reporting limit, meaning that the carbon filter was considered a non-hazardous waste. TCLP Sample 2, in the HEPA filter, showed that all metals were below the reporting limit except for lead, which was measured at 0.141 mg/L; the laboratory reporting limit for lead is 0.100 mg/L. This level corresponds to a non-hazardous amount of lead, as it is below the regulatory level of 5 mg/L as defined by U.S. Environmental Protection Agency Resource Conservation and Recovery Act regulations. The particle filter, which contained TCLP Sample 3, showed all metals were below the laboratory reporting limit except for lead and chromium, which were measured to be 464 mg/L and 0.302 mg/L, respectively. The chromium laboratory reporting limit is 0.100 mg/L, and the TCLP limit is 5 mg/L. Accordingly, the particle debris filter was determined to be a regulatory hazardous waste for lead. Therefore, this filter had to be disposed of and cleaned using the proper personal protective equipment for handling hazardous lead waste. However, it is noted that the LACR unit was not run to the point that the filtering systems were saturated and the system shut down or reached breakthrough. Accordingly, additional waste profiling of the HEPA and carbon filtering system components would be required upon scaled-up use of the system.

Surface Analysis

Analysis of the base, grit-blasted, and laser-cleaned material included optical and electron microscopy. Figure 19 shows the interface between the laser-cleaned surface and the coating that was present on the base material before cleaning. Optical microscopy shows the interface between the cleaned and exposed substrate and the paint.

Additional microscopy of the laser-cleaned surface showed that microscale regions existed where the red paint was still present (Figure 20). Some areas had high reflectance, and other areas appeared darker. These regions seemed to vary throughout the surface randomly. Using electron microscopy, it was observed that the reflective "shiny" regions of the surface were relatively flat and therefore could reflect ambient light more efficiently than the rougher, courser areas, which were much less reflective to visible light and therefore appeared dark. These qualitative observations were consistent with variations in surface topology as seen in the SEM, as shown in Figures 21 and 22.

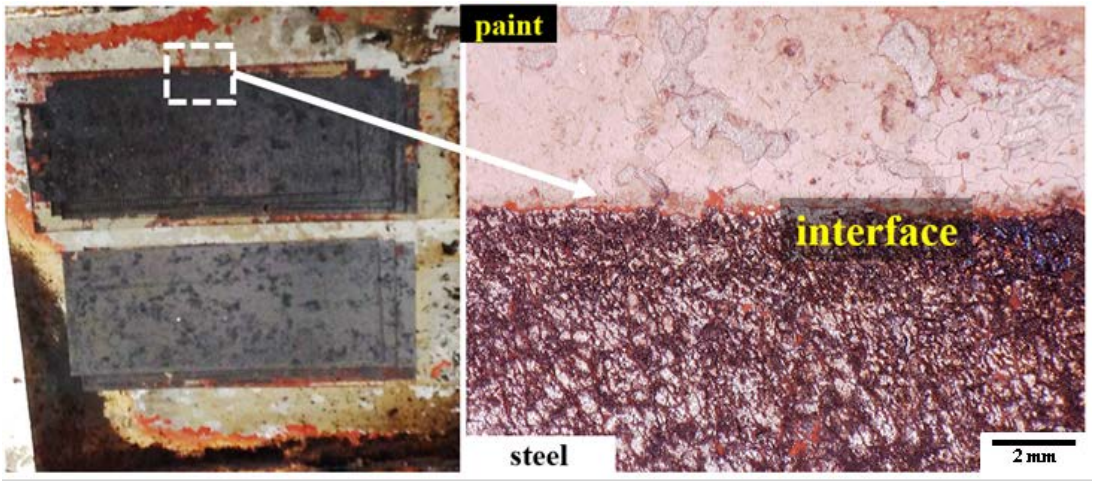

Figure 19. Views of Interface Between Painted and Laser-Cleaned Surfaces: (left) macroscopic; (right) optical microscopic

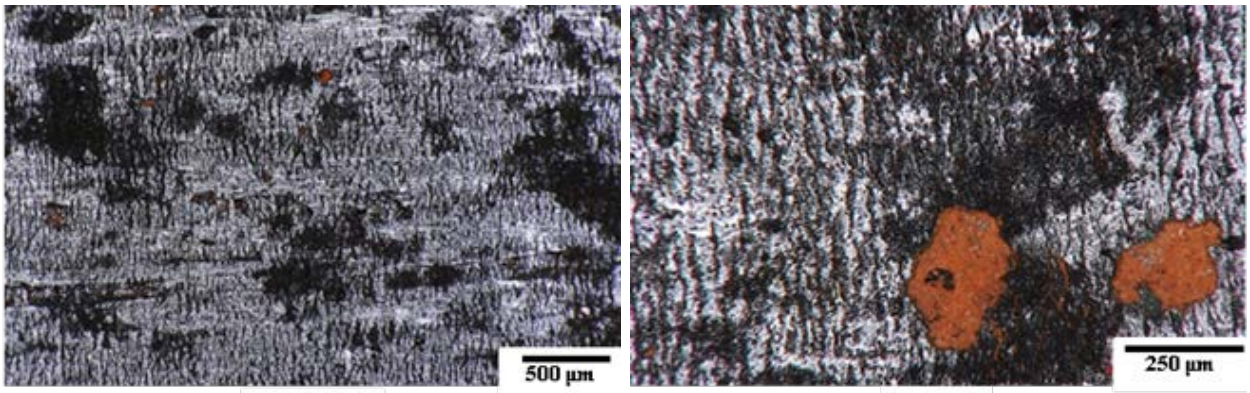

Figure 20. Optical Micrographs: (left) bright high-reflective surface and darker less-reflective areas; (right) clusters of red paint remaining on surface

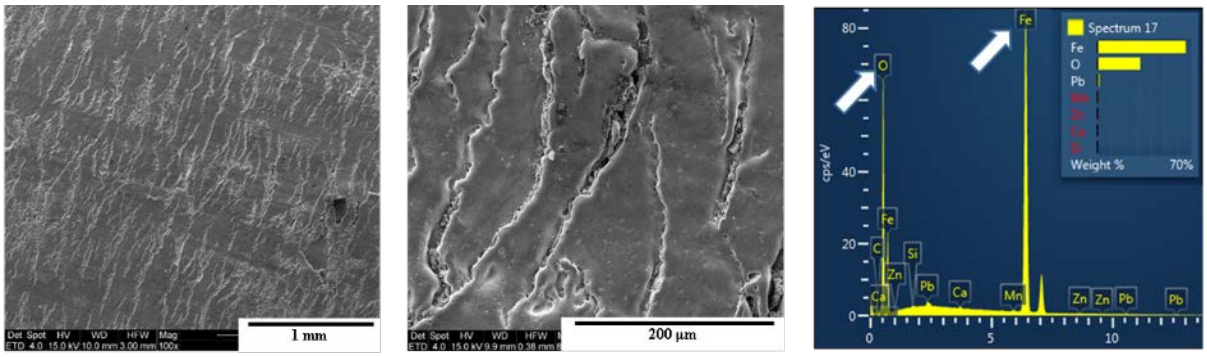

Figure 21. SEM Micrographs: (a and b) the laser-cleaned surface topology; (c) EDS spectrum indicating that mill scale dominates the majority of the surface shown. SEM = scanning electron microscope; EDS = energy dispersive spectroscopy.

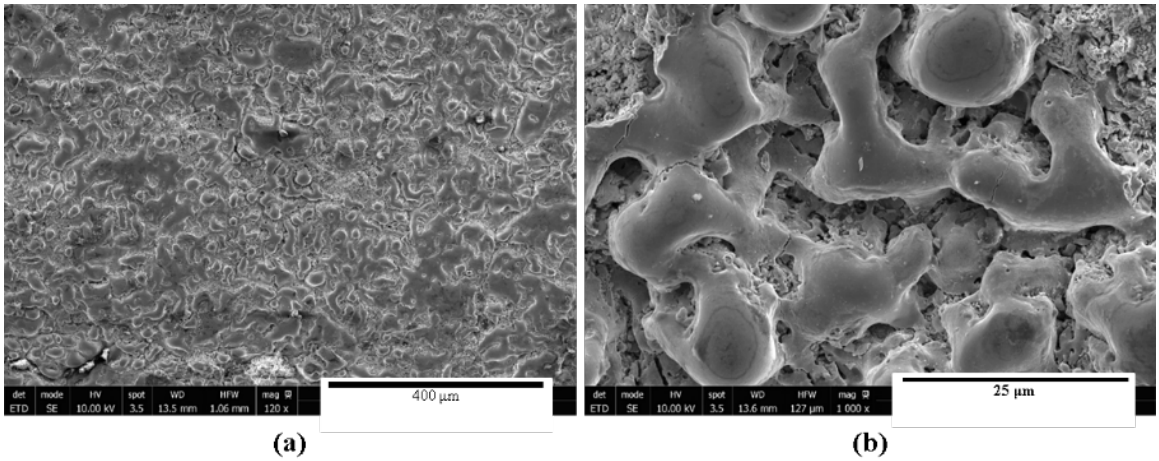

Figure 22. SEM Micrographs: (a) surface topology of surface regions containing the rougher surface profile; (b) higher magnification of region (a). SEM = scanning electron microscope.

Despite the shiny metallic appearance of the laser-cleaned surface, compositional analysis with EDS showed that the laser-cleaned surface consisted of iron oxide. At higher magnification, "mud" cracks were observed in the remaining iron oxide. Figure 22 shows how the rougher area contained raised areas, with valleys between these peaks, giving rise to the roughness of the surface.

Cross-Sectional Analysis

Cross-sectional analysis reveals information about the base material and the effects of the laser-material interaction. Scanning electron and optical microscopy of the base material shown in Figure 23 revealed that there were originally three layers of paint and a preexisting oxide layer prior to the laser-cleaning and grit-blasting decoating experiments. EDS analysis revealed that the base coating was a lead-based coating.

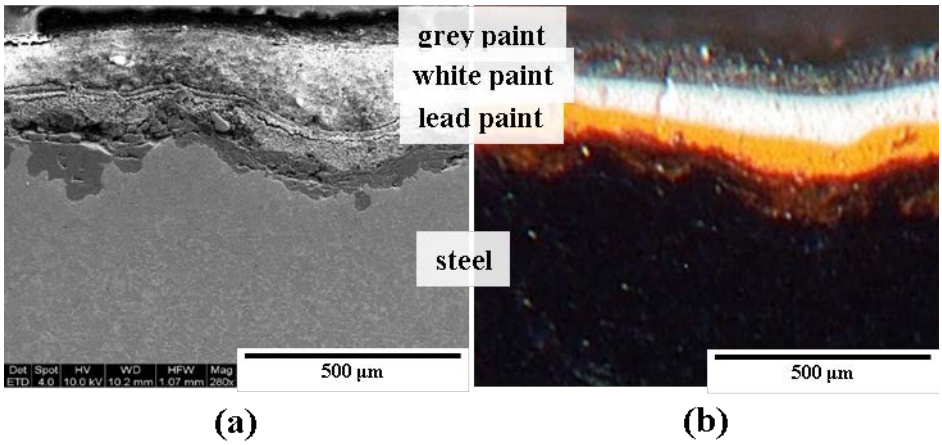

Figure 23. Cross Section of Base Material Showing Layers of Paint (or Coatings) and Iron Oxide: (a) SEM micrograph; (b) optical micrograph. SEM = scanning electron microscopy.

Cross sections of the laser-cleaned substrate also revealed the presence of a semi-continuous iron oxide layer, which varied from 20 to 100 µm across most of the surface, but that was not present in some regions. Figure 24 shows a cross section of the laser-cleaned substrate and the oxide layer that remained, including the melting of a thin surface region of the iron oxide, on the order of 1 µm or less in depth below the oxide surface.

The localized melting of the mill scale layer and exposed A36 steel surface was attributed to the local absorption by the paint and the metal at the fundamental laser wavelength (1064 nm). It is noted that there is some appreciable variation in the absorption depth of different materials depending on the wavelength. Given the compostion of A36 steel as a low carbon steel, a fairly low absorption skin depth on the order of 50 to 100 nm is expected for the wavelength employed in this study (1064 nm).

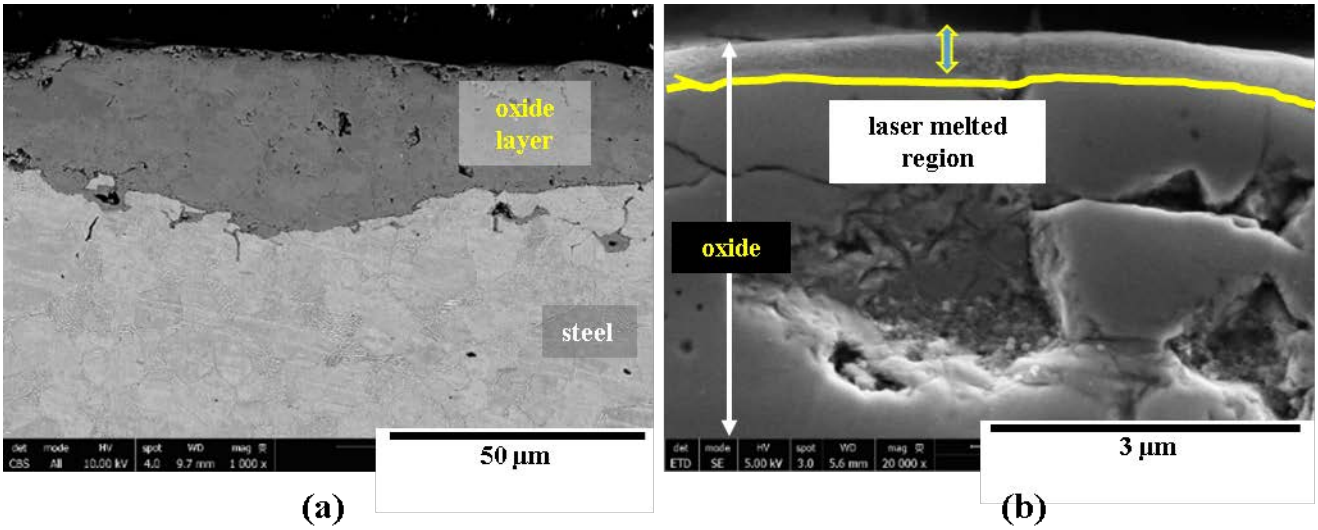

Figure 24. Cross-Sectional Analysis of Laser-Cleaned Surface: (a) iron oxide layer on surface; (b) higher magnification scanning electron micrograph showing melted surface region of the iron oxide layer

In regard to the coating system, removal by localized ablation and surface evaporation is common in the time regimes used here (nanoseconds). As noted previously, laser ablation uses high-energy pulses that are directed at a target to eject the surface layers of material. The effects of laser ablation can broadly be separated into three main categories; photothermal, where the heat generated by the laser pulse within the material dominates the interaction; photochemical, (photolytic), in which chemical processes dominate; and photophysical, in which both mechanisms contribute to the laser material interaction.[35, 36]

Given the level of organics in the coating systems, laser ablation of organic materials, specifically polymers, has been a topic of intense research since 1982, because of its many potential applications.[37-47] Laser ablation experiments involving pulsed lasers used both high and low frequency pulse settings.[48] Variations with laser scan speed and specific energy with duty cycle at different peak laser powers were also tried for steel alloy substrates. The general trend was that the laser scan (coating removal speed) increased with duty cycle as the pulse on-time and the input laser energy increased. It was found that there was a range of laser processing parameters that could be used to remove paint without damaging the substrate but that the process efficiency or specific energy was not the same over the entire range.

Multiple cross sections of the LACR samples helped to investigate the iron oxide layer that was left on the surface after LACR treatment. These cross sections helped reveal the origins of the two different surface topologies, i.e., the rough and the smooth regions. In the rough surface regions, the cross sections showed a tumultuous surface with peaks and valleys clearly observed. As seen on the surface, there was a variation in the shape of these features, as shown in Figure 25. It can be noted that the spacing and height of these peaks were different from one area to another, matching the observations from surface microscopy. In contrast, the smooth reflective parts of the LACR surface were lower in roughness, as expected. As shown in Figure 26, the microstructure of the underlying steel showed negligible signs of laser heating as evidenced by the unaltered pearlite ferrite grains right up to the oxide.

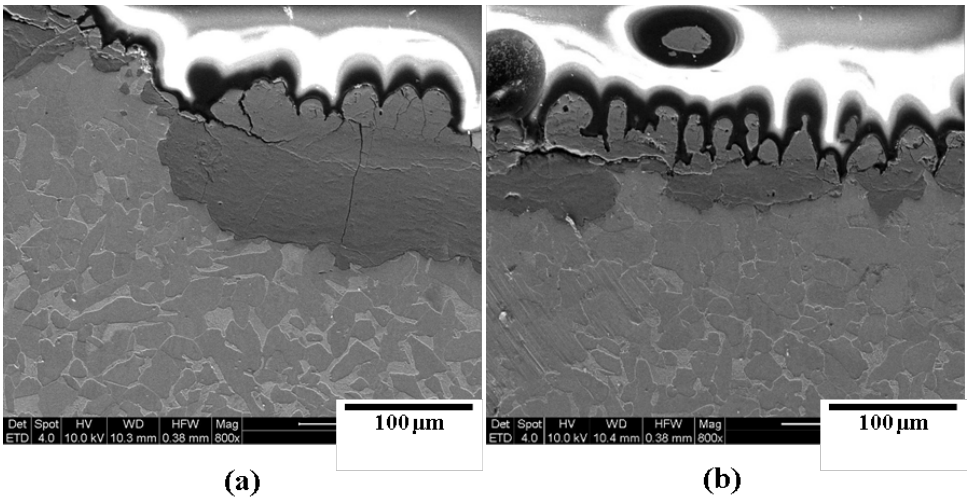

Figure 25. Cross-Sectional SEM Micrographs of LACR Sample Surfaces Showing Variation in Oxide Layer Surface Throughout One of the Rough Surface Regions: (a) oxide surface peaks are relatively spaced out compared to (b); (b) the distances between peaks decreased and the peak to valley heights increased. LACR = laser ablation coating removal.

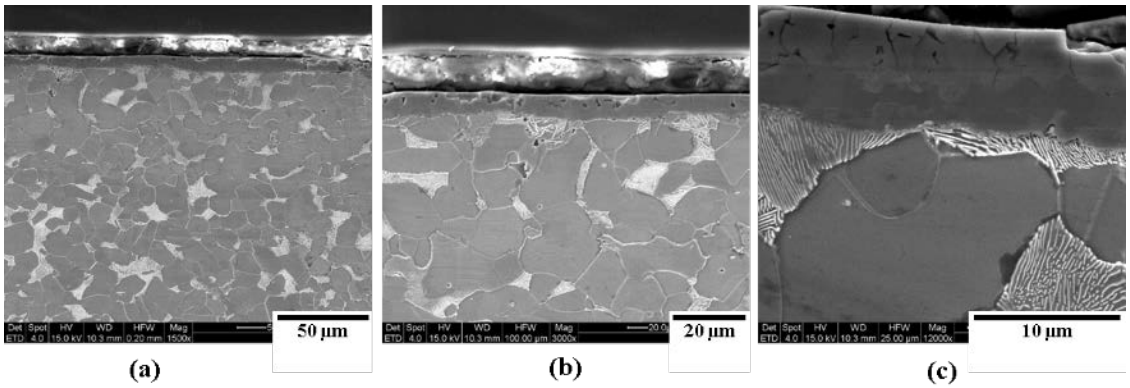

Figure 26. SEM Micrographs of LACR Sample Cross Sections Showing the Flat Oxide Surface Corresponding to: (a) reflective flat LACR surface regions; (b) higher magnification of (a); (c) high magnification SEM showing that the steel microstructure is consistent within the cross section to the oxide surface layer. SEM = scanning electron microscope; LACR = laser ablation coating removal.

As already mentioned, the iron oxide layer across the steel surface was not continuous at every point and in some places exposed the steel directly to the laser beam. In these regions, there was an effect on the surface that altered the appearance of the near surface region of the metal, along with the microstructure further into the steel. In Figure 27, an exposed part of the steel adjacent to an end of the iron oxide is seen in cross section, revealing the effect of the laser on the metal. At lower magnifications, the decrease in grain size compared to the bulk material can be seen. Highlighted with a red line (Figure 27c), a higher magnification image shows the near surface region affected by the laser.

Grit-blasted sample cross sections lack the oxide layer that was found on laser-cleaned samples. Instead, the near surface region of the cross sections revealed the deformation of grains because of the forces imparted to the metal during grit blasting. Up to a depth of roughly 10 µm, the grains were flattened and disfigured compared to the unaffected grains below them.

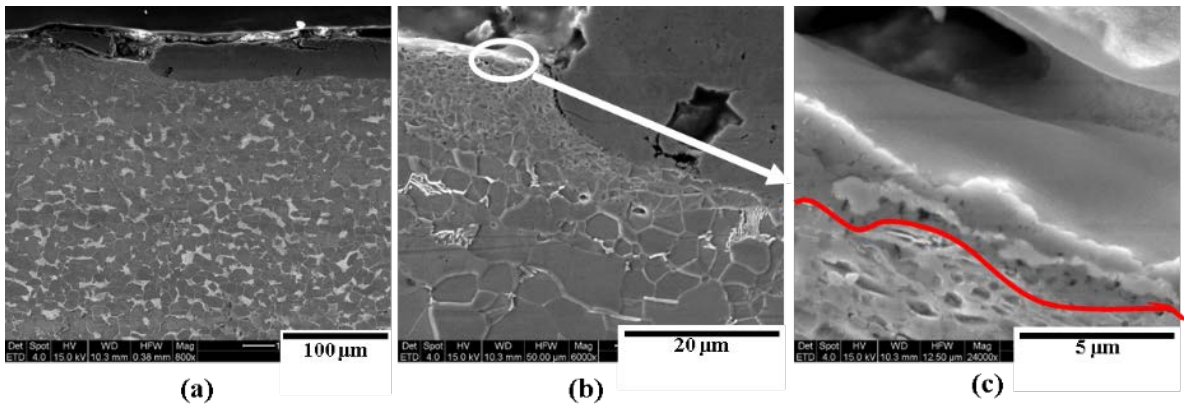

Figure 27. SEM Micrographs of LACR Sample Cross Section Showing Effects of Laser Damage Directly on Exposed Steel Adjacent to the Iron Oxide Surface Layer: (a) high-magnification micrograph showing effect of laser heat on near surface steel compared to bulk microstructure; (b and c) higher magnification micrographs showing the surface region affected by the laser heat, outlined specifically in red. SEM = scanning electron microscope; LACR = laser ablation coating removal.

Figure 28 shows SEM micrographs of grit-blasted sample cross sections and the near surface grains that were deformed because of grit blasting. Aside from the deformed grains at the surface, the roughness of the grit-blasted surface is implied by the high amplitude of peaks and valleys in the profile view of the cross-section surface. This is in contrast to the relatively smooth cross-section surface profile of the laser-cleaned samples.

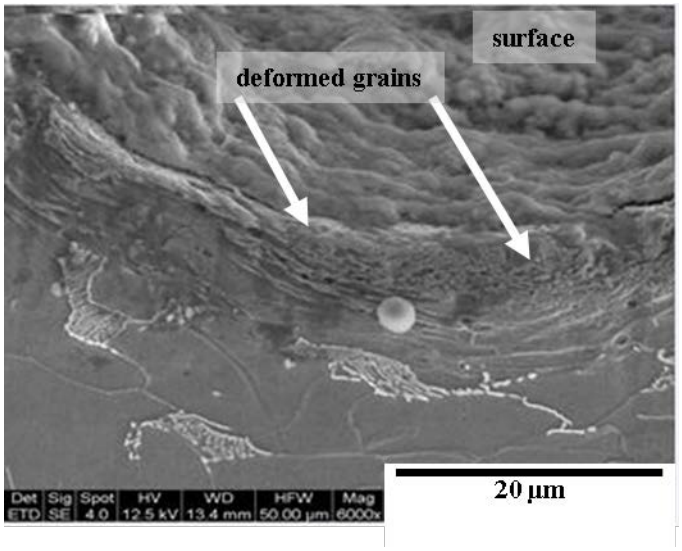

Figure 28. Grit-Blasted Sample Cross Sections Showing Deformed Grains in Surface Region

Coating Adhesion Testing

Because of the importance of coating bridge structures for protection, many state departments of transportation, including VDOT, have conducted research into various coating systems and their effectiveness.[49-52] One of the primary factors in the success of a coating in protecting the structural integrity of bridge steel is the adhesion of the coating to the metal substrate. Many factors can contribute to the adhesion strength, including the coating thickness, the coating system used, the environmental conditions at the time of the application of the coating,[53] and the surface condition of the substrate (such as roughness), among others. Although this study focused on the effectiveness of LACR for coating removal, coating adhesion is just as important because the metal must be recoated for corrosion protection.

Using the PATTI device, the adhesion of recoated epoxy mastic on laser-cleaned beams was assessed. The reapplied coating varied in roughness and thickness across different recoated beams and within beams themselves. Heavily applied coating left brush strokes easily visible, whereas thinner coatings seemed to be smoother. Upon testing these different regions, a correlation between the coating thickness and the adhesion strength of the coating was found, with a higher coating adhesion (2,094 psi) for thicker, rougher coated areas as compared with the thin areas (1,721 psi). These values were determined by averaging the pull-off tensile strength recorded for more than 50 pull tests for each coating condition and exceed VDOT requirements.[54]

Coating adhesion to substrates is mainly classified into several distinct mechanisms: adsorption, chemical, and mechanical adhesion.[55] Adsorption refers to the physical “bond” or

attachment between the coating and the substrate on the atomic level. This includes factors such as van der Waals forces that can keep polymeric or other organic binders in coatings adsorbed to the substrate surface. Chemical adhesion occurs when an actual chemical bond is formed between the coating and the substrate.[56] In mechanical adhesion, the liquid coating flows over the substrate surface filling holes, pores, crevices, and microvoids and then once hardened or cured achieves a mechanical grip to the surface. Mechanical interlocking with the surface is what provides the strength to the interface and accounts for why abrasive blasting or mechanical roughening is a common surface preparation treatment by providing a sufficiently rough surface for the coating to hold onto.[57]

In general, coating failure can be grouped into two types: adhesive failure and cohesive failure. Adhesive failure refers to a breaking of the bond between the coating and the substrate, whereas cohesive failure is when the coating or substrate itself mechanically fails, also resulting in ultimately breaking the coating substrate piece into two separate pieces. These two modes of coating failure are diagramed in Figure 29. Figure 30 shows SEM micrographs of the PATTI stub surface following testing. From these micrographs, residual coating and oxide are observed, along with remnant stub epoxy.

Overall, despite the presence of iron oxide on the steel surface, no detrimental effects from LACR on the coating adhesion properties of the substrate were observed. As discussed earlier, the oxide layer may even act to enhance the coating adhesion, providing a bond to the epoxy paint that is stronger than the adherence between the iron oxide and the steel itself.

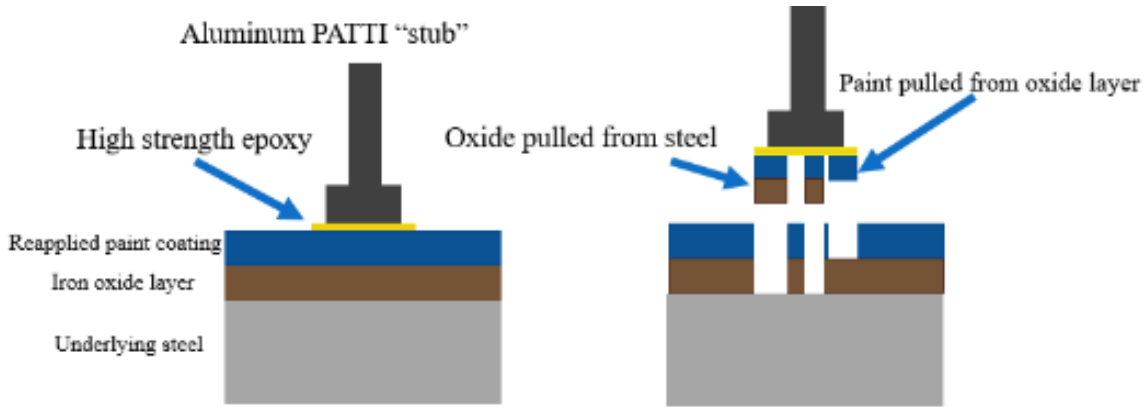

Figure 29. Diagram Showing How PATTI Test Stubs Removed Reapplied Paint From Surface Oxide and Oxide From Underlying Steel. This implies that the paint-to-oxide bond can be stronger than the oxide-to-metal interface. PATTI = pneumatic adhesion tensile testing instrument.

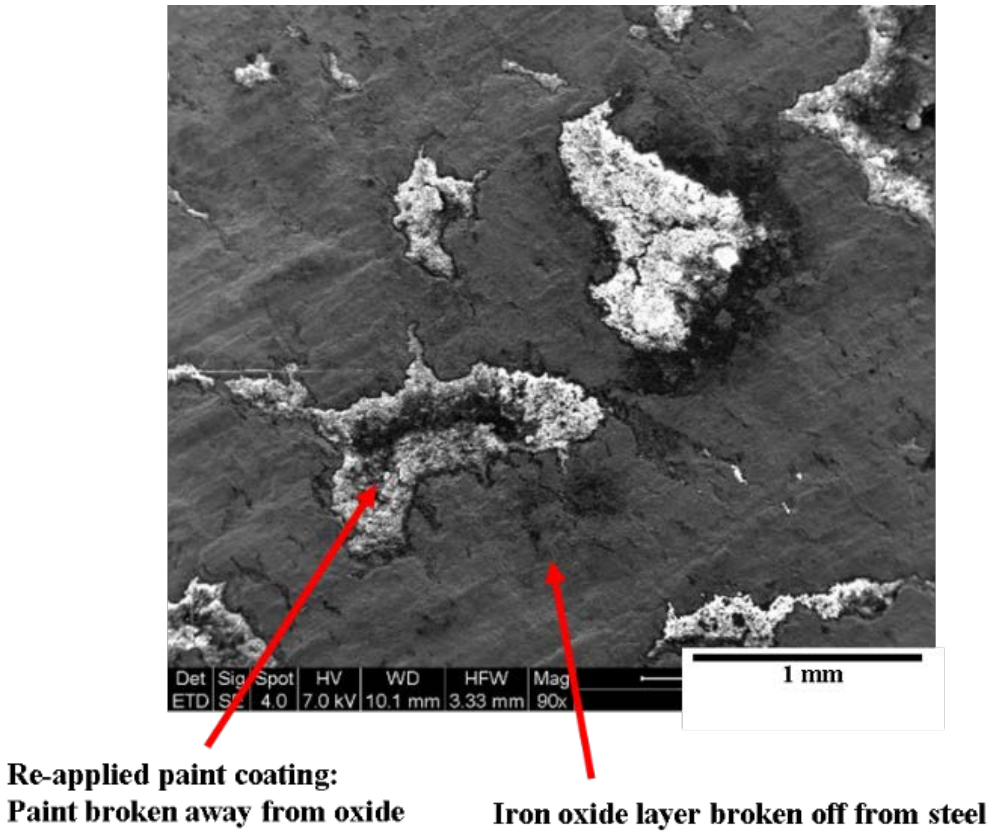

Figure 30. SEM Micrographs of PATTI Stub Surface After Testing. Iron oxide and residual paint were observed. SEM = scanning electron microscope; PATTI = pneumatic adhesion tensile testing instrument.

Surface Roughness

Using a surface profilometer, the surface roughness of different processed surfaces was investigated. The biggest variable for surface roughness was the abrasive-blasted surface condition versus the laser-cleaned surface. Besides the difference in processing condition, for the laser-cleaned surface there are laser tracks present from the laser surface interaction. The abrasive-blasted surface had a rougher profile, with an average roughness value of 9.86 μm. Both laser-cleaned surface measurements had lower average roughness values, of 5.41 μm and 5.26 μm, for the profiles perpendicular and parallel to the laser tracks, respectively.

Mechanical Behavior

Hardness

Vickers hardness tests were performed on samples in the as-received, abrasive-blasted and laser-cleaned conditions. Hardness was measured as a function of depth into the material from the processed surface, at roughly 75-μm intervals. Ten hardness measurements were made at each depth into the steel and averaged. Figure 31 shows the hardness results for the three different processing conditions.

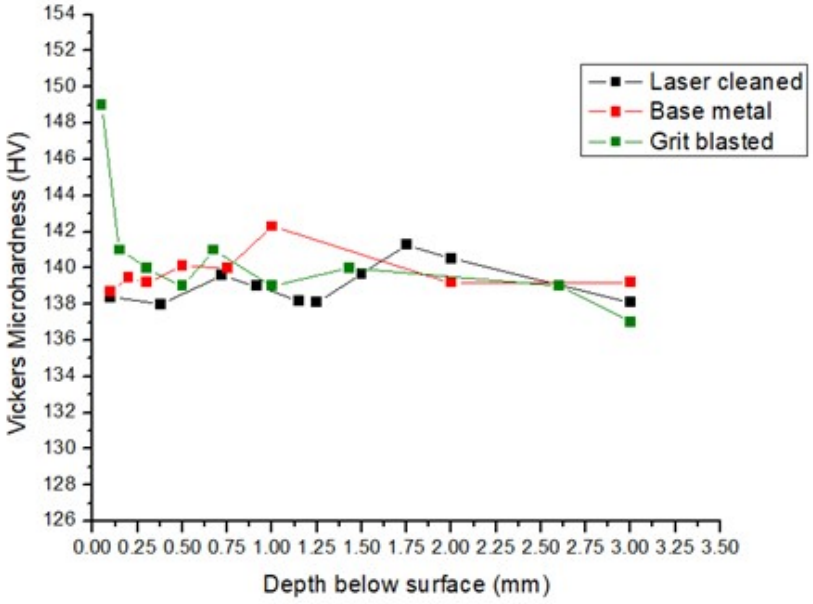

Figure 31. Hardness Profile of All Three Processing Conditions From the Surface Into the Bulk of the Material

The base metal showed little variation in hardness with depth, with an average hardness of approximately140 HV. Laser-cleaned metal also showed essentially no change in hardness with depth. Cross-sectional analyses showed that the near surface region was heated and melted (to a depth of approximately 1 μm); however, the underlying metal seemed to be unaffected by the heat. In contrast, grit-blasted samples had a higher hardness near the surface (149 HV), but the hardness quickly decreased and then remained similar to the base metal values. The elevated hardness at the surface is was due to the deformation imparted by the grit blasting.

Tensile Strength

Tensile testing was completed on base metal, abrasive-blasted, and laser-cleaned samples to determine the effects of different processing conditions on the strength of the metal. Laser ablation had negligible effects on the strength, as all three processing conditions showed the same yield and ultimate tensile strength of 41 ksi and 64 ksi, respectively (Figure 32), which matched the mechanical properties of A36 steel, which has a minimum yield strength of 40 ksi and an ultimate tensile strength ranging from 58 to 80 ksi.[58] Further, no appreciable differences in the ductility were found, with all samples falling between 30% and 40% elongation vs. the minimum value of 23% for A36 steel.

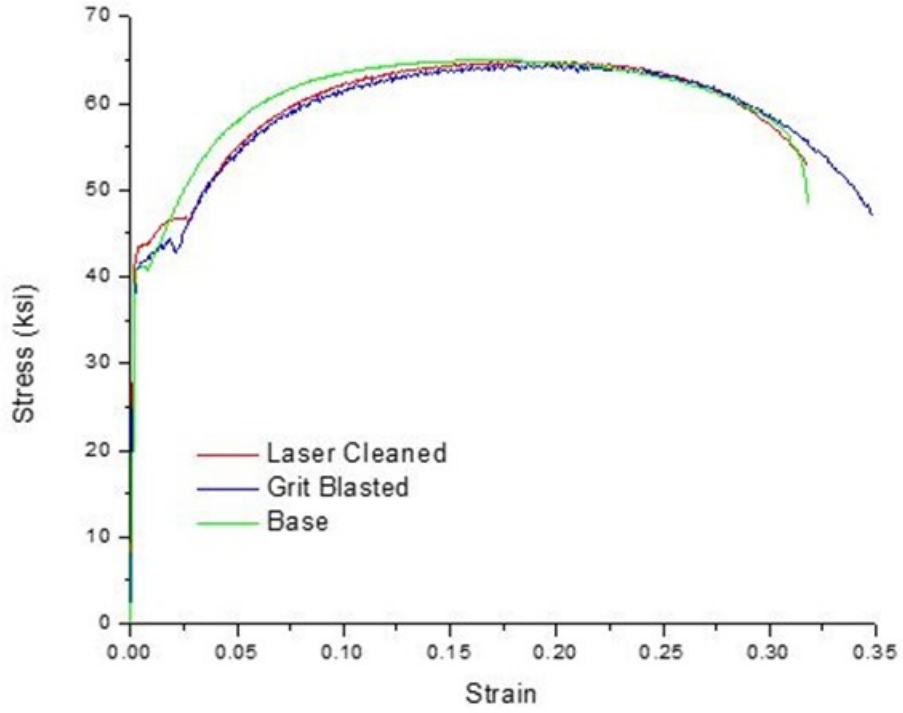

Figure 32. Stress Strain Curves for Base, Grit-Blasted, and Laser-Cleaned Metal

Fatigue Strength

Testing was performed to investigate the effect of laser ablation on the fatigue life of the steel. Although the endurance limit was not rigorously determined, the fatigue results in Figure 33 show that it was in the range of 44 ksi (for R = 0.1). A review of the literature showed A36 steel to possess an endurance limit of 39 ksi under fully reversed loading conditions (R = -1).[59] Detailed fractographic analysis of the current steel, manufactured in 1932 or before, revealed extensive manganese sulfide (MnS) inclusions, which are known to be a source of embrittlement in steels.

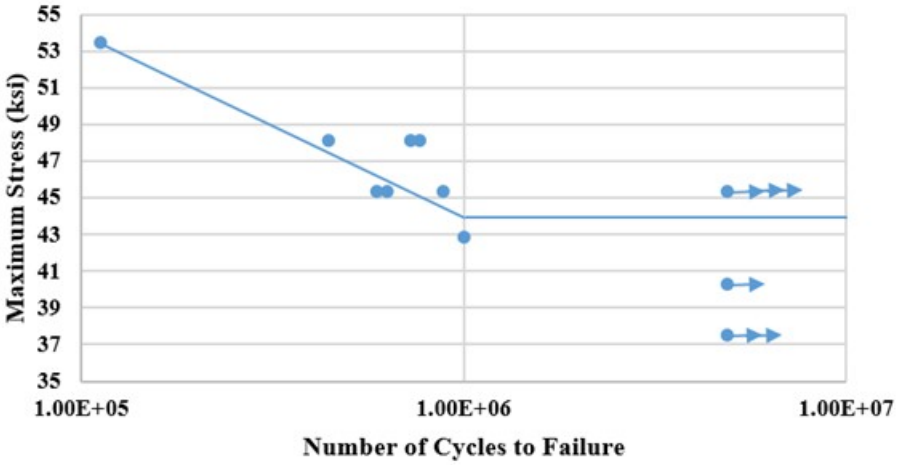

Figure 33. Plot of Stress (S) vs. Number of Cycles to Failure (N), or S-N Curve, for LACR Fatigue Sample. Arrows on points at 5×10^6 represent run-out tests. LACR = laser ablation coating removal.

Fatigue lives are composed of an initiation and propagation phase. The hardness and tensile test results showed that the effects of LACR on the mechanical properties were restricted to a very near-surface region. Therefore, the effect on fatigue was anticipated to be most clearly observed in the initiation phase, since cracks initiate most frequently on the surfaces of the samples. Figure 34 is an SEM image of the fracture surface. It reveals that the final fracture was a result of linkage of numerous microcracks, which initiated on the surfaces of the samples. Observations of the outer surfaces of the fractured samples revealed numerous secondary cracks on both sides of the samples, those that had been subjected to LACR and those that were surface ground as a control case. In fact, samples did not show a likelihood for initiation on the side of the sample that had been subjected to LACR.

Finally, it is noted that previous fatigue testing on a similar, present-day alloy, DH36, in both LACR and grit-blasted conditions revealed an endurance limit of 23 ksi to 30 ksi (again at R = 0.1).[19] A detailed analysis revealed that this wide range of behaviors was dependent upon the thermomechanical treatment employed by the steel vendor and upon the surface treatment applied prior to LACR. These tests showed no universal reduction in fatigue performance after LACR. Rather, the results showed that the fatigue properties were more strongly dependent on the prior surface treatment (i.e., how aggressive a grit blasting was performed).[60]

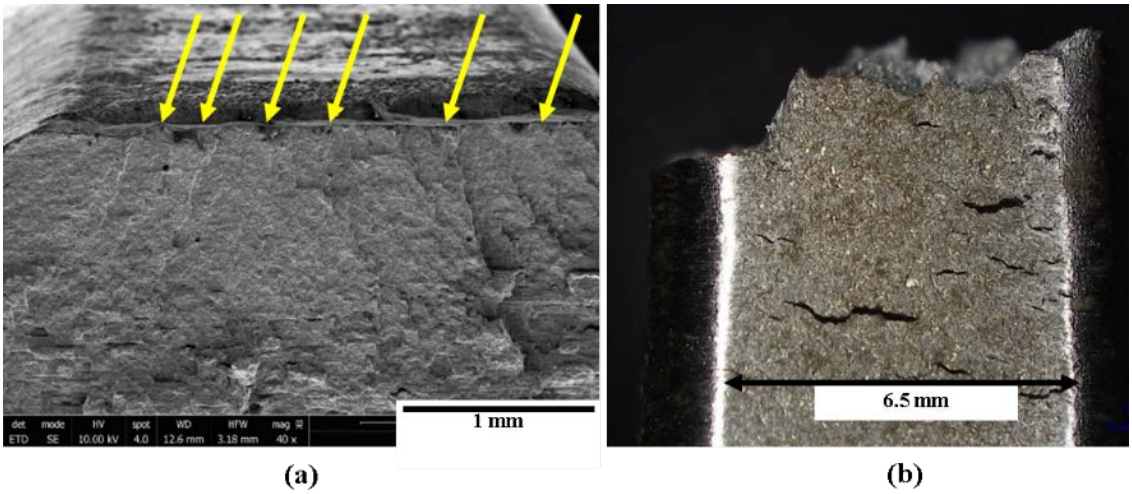

Figure 34. SEM Image of Fracture Surface: (a) direct view of crack propagation from iron oxide surface layer through to the bulk material showing the interaction of the crack growth and the inclusions; (b) view of sample side showing multiple cracking seen on all sides. SEM = scanning electron microscope.

LACR Phase 2: Field Demonstration

Phase 2 consisted of an on-site demonstration of the feasibility of using the LACR system on an in-service bridge structure. The bridge selected was along Route 695 in Prince Edward County, Virginia, near Farmville. After a 2-day delay because the generator at the site was not providing sufficient voltage, i.e., 325 V measured output rather than the required 480 V, and poor weather conditions, the laser testing started on August 16, 2017. Figure 35 shows the underside of the bridge where the LACR cleaning was being performed.

Figure 35. Laser Ablation: (a) LACR system in use to clean a component of the beam end; (b) exposed surface after laser ablation; (b, c, and d) representative images of beam ends that could not be reached with the laser for cleaning. LACR = laser ablation coating removal.

Phase 2 showed that deployment and operation of the LACR system to remove bridge coatings in the field were possible. It also revealed, however, some shortcomings with LACR. Although cleaning of open flat areas of the I-beams worked, removal of the coating was slow. The coating had been in service for about 44 years, with measurements indicating a thickness of approximately 6 mils on the girders and approximately 11 mils on the cross frames.

During Phase 2, it also became clear that the beam ends, cross frames, and bearings had regions that were inaccessible because of the limited space and tight geometries in the areas adjacent to the bridge's backwall. An earlier presentation by the manufacturer of the LACR equipment had shown adapters that allow for coating removal in tight spaces. It was evident from the design of the laser head and the geometry of the power and vacuum cable that access to specific areas of the structure would be challenging (Figure 35b, c, d). It was not possible to clean these parts of the beams, cross frames, or bearings, which are higher priority areas for cleaning because of excessive corrosion damage that occurs in these locations, as discussed previously. However, the LACR system was able to clean more easily accessible features in the field (Figure 36).

Figure 36. LACR System During Cleaning: (a) cables exiting back of laser optic; (b) portable generator and on-site cables. LACR = laser ablation coating removal.

Upon completion of the field study, the inspector estimated that approximately 50 ft^2 of surface area had been coated with a coating that met VDOT specifications for Coating System F. The coating system was an Epoxy Mastic Aluminum II primer with an Acrolon 218 HS finish coating. The inspector also noted that although the laser ablation process was extremely clean and favorable for workers and the environment, the coating removal rate was slow. The inspector highlighted that cleaning behind the girders, shoes, bearing, and diaphragms was time-consuming for LACR but that the equipment supplier suggested that other LACR equipment was available that could reach these areas.

Industrial Hygiene

IH testing was also performed during this phase of the study. Personal sampling devices were worn by the two laser operators. The lead concentration was 21 $\mu g/m^3$ for Operator 1 and 8.4 $\mu g/m^3$ for Operator 2. Based on these results, exposure over the work shift did not exceed the AL. Table 5 summarizes the PEL and AL for the nine metals surveyed and collected in the area and the personal samples.

The area air samples were gathered at 25 ft below the bridge in the area of the laser operation, 14 ft east of the work area, 14 ft west of the work area, and 2 ft from the filter unit exhaust. All samples were below the level of detection except the exhaust sample, which detected lead at 0.86 $\mu g/m^3$.

Environmental Compliance

During the field study, the waste material generated was considered hazardous based on 2017 historical TCLP testing results. The HEPA filter exceeded the regulatory waste requirements for lead and the particle debris filter for lead and chromium.

LACR Phase 3: Cleaning Tight Geometry Demonstration

Phase 3 was conducted to investigate the ability of LACR to remove coatings effectively from areas that are difficult to access, such as bridge beam ends and bearings. This demonstration took place on November 9, 2017, with a bridge bearing that was provided by VDOT. The bridge component was evaluated at the facility of the LACR representative in Chesapeake, Virginia. The bearing is shown in Figure 6 and Figure 37.

The 500W system with the CleanCUBE head appeared to remove most of the outer layer of rust and remaining paint after multiple passes; the 1000W system was also tested. After the vacuum nozzle was removed to shorten the laser optic head length, the 1000W laser was tested, leaving a surface comparable to that observed after cleaning with the CleanCUBE head. However, even with the vacuum nozzle on the 1000W optic laser head removed, the optic was still too large for use in cleaning bridge beam ends and bearings. Therefore, the 500W system with the CleanCUBE head was determined to be the only viable option for cleaning these tighter and recessed areas. Figure 37 shows photographs of the bearing component before and after both the 500W and 1000W systems were used to remove the coating. Although this figure illustrates the benefit of using both systems together, the locations cleaned by each system were not documented.

Recalling the speed of operation findings from Phase 1 is useful at this point. The measured difference between operating speed with and without the roller represents the speed cost to an operator who must maintain the proper distance by hand and eye alone. It provides also an intuitive explanation for the observed—although not clocked—slower rate at which operators were able to remove paint from corners and angles where a roller could not be used during Phase 3.

(a) (b)

Figure 37. The Bearing (a) Before and (b) After Laser ablation Using the 500W and 1000W Laser Systems

LACR Phase 4: LACR Removal Before Hot Work

VDOT conducted an IH survey on July 30 and August 1, 2018, to investigate using LACR to abate hazardous coatings prior to hot work. Two beams were removed from a decommissioned bridge and transported to the facility of the LACR representative to have LACR performed. These beams are shown in Figure 38, which shows different stages of the cleaning operation. While this work was performed, it was observed that maintaining contact between the roller and the steel during LACR resulted in the best air quality and greatest efficiency during coating removal. After the coating was removed from several sections, the beams were moved to a VDOT yard to have hot work performed.

(a)

(b)

(c)

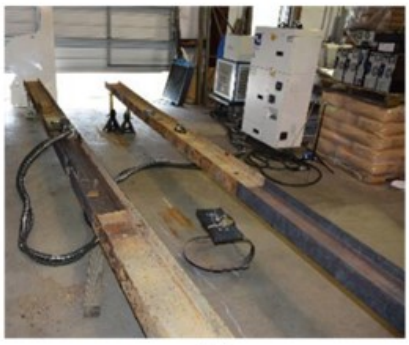

(d)

Figure 38. The Two Beam Styles Before and After LACR: (a) beams prior to cleaning; (b) end of the I-beam that was labeled Beam A; (c) end of the welded C-channel beam that was labeled Beam B; (d) beams after cleaning with LACR before hot work was performed. LACR = laser ablation coating removal.

The hot work included spark-generating tasks such as grinding, oxyacetylene torch cutting, and plasma torch cutting, which can be seen in Figure 39. It was clearly evident during this stage that the C-channel beam exhibited less predictable behavior during the cutting operations because of the material trapped between the surfaces of the steel. The deposits that were trapped between the steel surfaces (Figure 38c) were not removed by LACR. This was not surprising since LACR will not pass through the steel to remove trapped debris; therefore, these trapped materials were subjected to the subsequent hot work process when it was performed.

Figure 39. Various Hot Work Processes Being Performed on Beams After LACR: (a) Beam A being cut with an oxyacetylene torch in an area cleaned using LACR; (b) grinding after coating has been removed using LACR on Beam A; (c) plasma torch cutting in same cleaned area. LACR = laser ablation coating removal.

Industrial Hygiene

LACR Removal

During LACR, personal samples were below the level of detection for lead, cadmium, chromium, hexavalent chromium and PCBs. Area samples at the end of the two beams during LACR, near the exhaust, showed a concentration for lead of 7.2 $\mu g/m^3$, which was below the level of detection for cadmium and chromium.

Hot Work

Personal samples collected during hot work were short duration samples for lead. For oxyacetylene torch cutting on Beam A, the lead concentration was 56.3 $\mu g/m^3$ and for Beam B was 226 $\mu g/m^3$. For plasma torch cutting, the lead concentration was 29.2 $\mu g/m^3$ for Beam A and 152 $\mu g/m^3$ for Beam B. For surface grinding, lead concentrations for both Beam A and B were below the level of detection, $<14.5\ \mu g/m^3$ and $<22.3\ \mu g/m^3$. These measurements employed NIOSH Method 7300. As noted previously, the NIOSH manual states that the "Percent RSD" (the confidence interval) is ±6.12 percent or lower, depending on the filter medium selected for the test.

VDOT's Environmental Division provided for comparison six lead measurements from the personal air filters of the operators cutting painted steel beams with oxyacetylene torches. Two of these, yielding values of 5,298 $\mu g/m^3$ and 15,286 $\mu g/m^3$, were obtained by NIOSH Method 7082, with an accuracy as stated in the manual of ±17.6%. Four of these, yielding values of 11,900, 19,900, 22,800, and 5,800 $\mu g/m^3$ were obtained by NIOSH Method 7300. From these samples of sizes N1 = 6 and N2 = 2, one can compute a t-test of the hypothesis that the means are equal. The t statistic that resulted from this comparison of the means had a value of 2.030; the hypothesis that the means are equal is rejected at an 8.8% level of confidence, with prior LACR of the coating appearing to reduce significantly the level of lead liberated during hot work.

VDOT's Environmental Division also provided one sample from the personal air filter of an operator engaged in a combination of preparatory grinding (i.e., cleaning) of a painted steel beam and torch cutting subsequent to the grinding: the lead concentration in this air sample, 966 $\mu g/m^3$, is believed to be a composite of the comparatively high level that would prevail during the preparatory grinding and the comparatively low level that would prevail during the torch cutting after grinding; if measured during grinding only, the lead concentration would presumably be higher. A sample of size N = 1 will not permit a statistical test, but the reader will note that the lead concentrations measured during grinding after LACR are 2 orders of magnitude lower than the lead concentration measured during grinding when grinding itself was the method of paint removal.

Although this work showed that the laser ablation process can be used successfully to prepare a coated beam for hot work (i.e., torch cutting, welding, and grinding) in a manner that reduces the risk of employee exposure during routine hot work operations, care should be taken to ensure that the laser is able to access and remove the coating. It is also important to note that

extended cutting operations could expose the worker to lead levels over the AL and procedures for conducting this work are outlined by the VDOT Lead Exposure Control Program.

Surface Analysis Results

After VDOT performed its investigations, cut sections of the I-beams were transported to UVa for further surface characterization. After smaller (roughly 1 in x 1 in) metal samples were cut out from the I-beams, the surfaces were studied with the SEM and by XRF, with the primary goal of measuring the remaining amount of lead on the surface. Figure 40 shows SEM micrographs and accompanying EDS data for the surface region shown. As expected, EDS show a high content of iron and oxygen. The weight percentage of iron (Fe) from EDS typically fell within the 70 to 80 percent range, and that of oxygen (O) approximately around 15 percent. Aside from these two dominant elements, smaller amounts of other elements such as C, Cl, Mn, and Na were also present. Regarding lead, the element under investigation, it consistently appeared in EDS analysis but only in trace amounts. In fact, EDS data analysis consistently placed lead at the bottom of the list of trace elements. This finding is consistent with the results of the lead wipe tests and prior chemical analysis performed by the contractor.

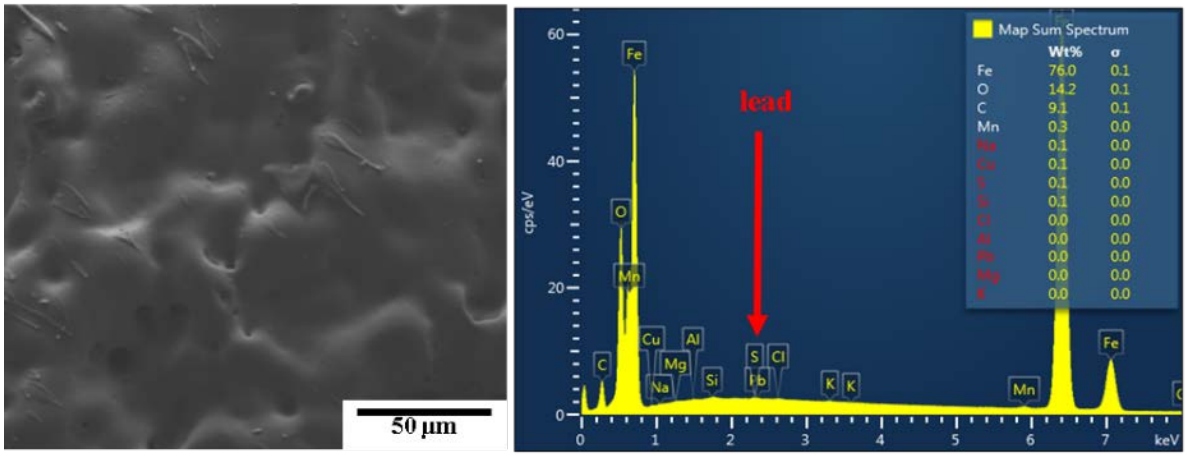

Figure 40. SEM Micrograph and EDS Data: (a) LACR-cleaned surface; (b) EDS spectra showing that Fe, O, and C were the main elements present in the composition of the surface, with remaining elements in trace amounts. SEM = scanning electron microscope; LACR = laser ablation coating removal; EDS = energy dispersive spectroscopy.

LACR Phase 5: TFHRC Steel Surface and Coating Evaluation

Evaluation of Uncoated Phase 1 Steel Samples

Yield and Ultimate Tensile Strength Testing

Tests were run on a 25 kip MTS servo-hydraulic test frame using hydraulic wedge grips. A calibrated MTS strain extensometer was used to span a 1-in-gauge section of the dog bones. The tests were run under automated control using MTS's TestSuite software. Load and strain

rates were set in accordance with ASTM E8. The tensile test results are provided in Table 6. Specimens 1 through 7 were tested, with the rest of the specimens reserved as spares. The test for Specimen 4 was not considered valid, as the specimen broke outside the gauge section being measured by the extensometer. Based on the measured yield and tensile strength results, which were consistent among the steel beam samples tested, these values are reasonable for a typical A36 low carbon steel.

Table 6. Measured Yield and Tensile Test Data for Specimens 1-7

Specimen No.	Measured Yield Strength, lb	Measured Tensile Strength, lb
1	43,000	67,330
2	41,000	65,160
3	42,000	67,047
4[a]	43,100	68,958
5	41,000	60,406
6	39,000	60,403
7	39,000	60,810

[a] Specimen 4 was included for completeness, but the test was considered invalid since the specimen broke outside the gauge section during testing.

Composition of Steel

Using a Leco Spark Spectrometer, the composition of the steel used in Phases 1 and 5 was determined. The results are provided in Table 7. The numbers for each element correspond to the reference sample used by the spectrometer in making the elemental match. Based on the chemical analysis, it was concluded that the steel is a typical A36 low carbon steel.

Table 7. Chemical Analysis of the Two Beam Materials

Element	C165 %	Mn403.0 %	Si288 %	P177 %	S180 %	Cr Calc.	Cr301.4 %	Cr357 %	Ni341 %	Mo386 %	Cu327 %	V411 %
Narrow beam	0.302	0.471	0.051	0.022	0.039	0.103	0.099	0.103	0.008	0	0.069	0
Wide beam	0.202	0.621	0.032	0.01	0.025	0.067	0.122	0.067	0.094	0.014	0.235	0.001
Element	**Al396 %**	**Ti334 %**	**Sb206 %**	**Nb405 %**	**Co340 %**	**W400 %**	**B208 %**	**Ca393 %**	**Zr360 %**	**As189 %**	**Sn326 %**	**Fe249 %**
Narrow beam	0.021	0	0	0.005	0	0.01	0	0.003	0.029	0.144	0.017	98.71
Wide beam	0.01	0	0.007	0	0.003	0	0	0	0.009	0.034	0	98.58

Surface Profile Evaluation

Examples of the surface profiles, as observed under an optical microscope, can be seen in Figure 41. Some surface areas of the beams were visibly rough because of corrosion. The uneven surface areas with deep pits and gorges were not suitable for measuring the surface profile, which is defined as the peak-to-valley depth that is created during surface preparation. Therefore, the surface profile data represent the areas that were relatively even and flat at the macro level.

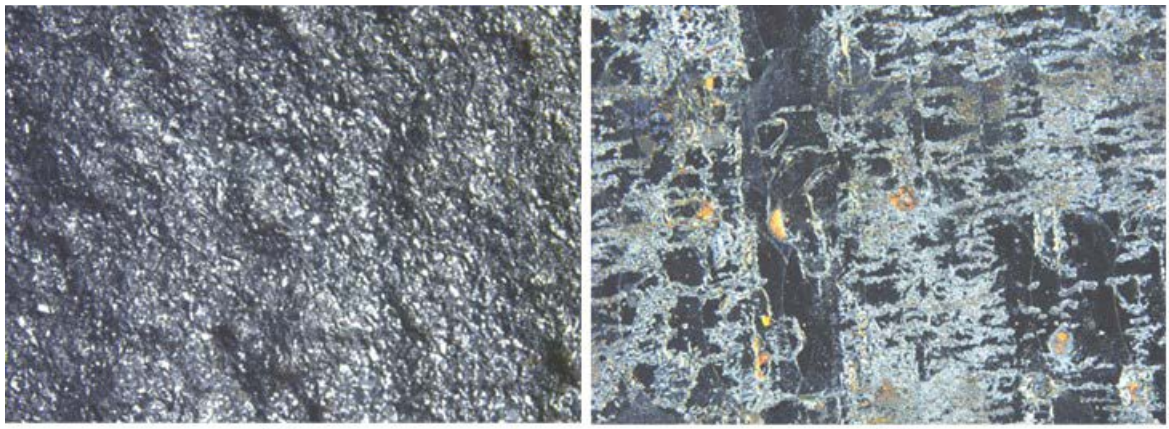

Figure 41. Optical Micrographs: (a) grit-blasted surface; (b) laser-cleaned steel surface

Staff at TFHRC measured the surface profile of the steel panels with a surface profile gauge in accordance with ASTM D4417, Standard Test Methods for Field Measurement of Surface Profile of Blast Cleaned Steel, Method B: Surface Profile Depth Gauge. As shown in Table 8, the grit-blasted 5-ft beam had a surface profile of 3.5 mils and the laser-cleaned 5-ft beams had a surface profile of 2.3 mils. In each case, the standard deviation was 0.9 mil. On the assumption that the sample size in each group was N = 10 (ASTM D4417 prescribes a measurement sample size of 10 or more), the t statistic that resulted from a comparison of the means had a value of 6.667; the hypothesis that the means are equal is rejected at a 2.9×10^{-6} level of confidence; laser ablation appeared to create a shallower surface profile than grit abrasion. Table 9 shows the surface profile of the 1-ft beam sections.

Table 8. Surface Profile of 5-ft Beam Sections

Steel Substrate	Average, mil	Standard Deviation	Max.	Min.
Grit blasted	3.5	0.9	5.0	0.8
Laser ablated	2.3	0.9	5.1	0.1

Table 9. Surface Profile of 1-ft Beam Sections

Section	Average, mil	Standard Deviation	Max.	Min.
1A	2.4	1.1	4.9	0.8
2A	3.0	1.0	5.0	1.2
3	1.9	1.0	4.5	0.4
5	4.1	0.6	4.9	3.4
8	2.6	1.0	5.0	1.1
10	2.6	0.9	4.7	0.8
11	2.7	1.1	4.8	0.6
12	3.0	1.0	4.9	0.8
13	4.1	0.5	4.9	3.5
14	4.0	1.5	4.9	2.2
18[a]	2.6	1.0	5.0	0.7
19	2.9	1.0	4.8	1.1
Average	3.0			

[a] Grit blasted.

Soluble Chloride Analysis

During the soluble chloride analysis, multiple samples were collected from the 5-ft-long beams, as shown in Figure 42, and the shorter 1-ft samples as shown in Figure 43, which also shows the extraction setup.

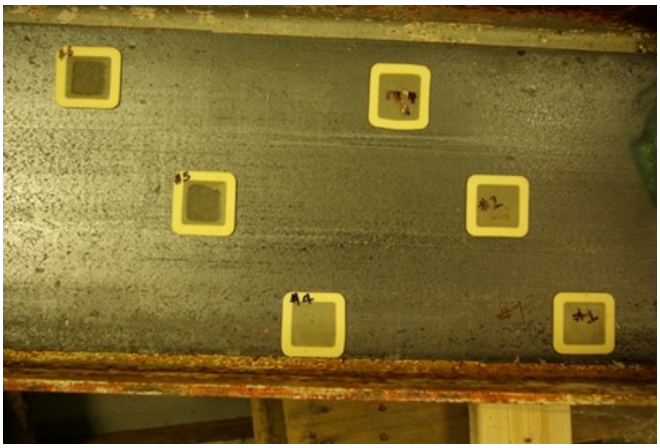

Figure 42. Multiple Samples for Soluble Salt Analysis Collected From Surface of the 5-Ft Beam

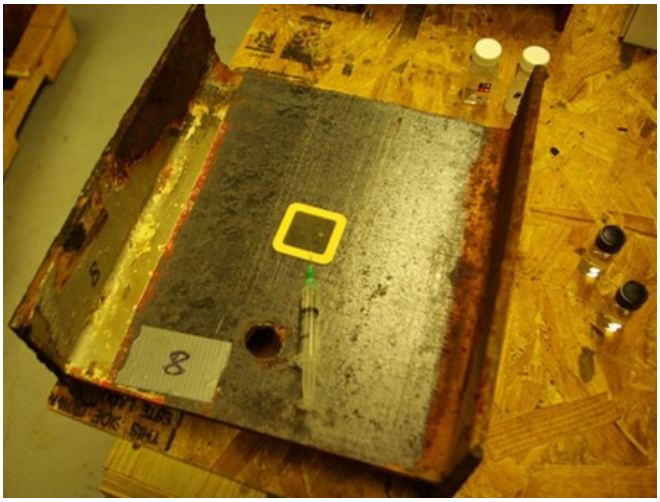

Figure 43. Samples for Soluble Salt Analysis Collected From Surface of the Shorter 1-Ft Beams. The extraction process can also be seen.

The results for the 5-ft beams are shown in Table 10. The soluble chloride content varied among different locations on the same beam, but the average value of the two beams was similar: the grit-blasted beam had an average chloride content of 1.0 µg/cm^2, and the laser-cleaned beam 0.9 µg/cm^2.

Table 10. Chloride Contamination on Laser-Cleaned or Grit-Blasted 5-ft Beam Sections

Test Location	Surface Density, μg/cm^2	
	Grit Blasted	Laser Cleaned
1	0.9	0.7
2	0.7	0.4
3	0.6	0.3
4	0.6	0.7
5	0.7	1.5
6	0.9	0.5
7	1.6	1.4
8	1.6	1.5
9	1.5	1.5
Average	1.0	0.9

For the nine grit-blasted locations, the mean chloride concentration was 1.011 μg/cm^2 and the sample standard deviation was 0.431. For the nine laser-cleaned locations, the mean chloride concentration was 0.944 μg/cm^2, and the sample standard deviation was 0.520. The t statistic that resulted from a comparison of the mean chloride concentrations in Table 10 has a value of 0.628; the hypothesis that the means are equal cannot be rejected.

The results for the chloride content on the 12 1-ft beam sections is shown in Table 11. The average surface content was 0.5 μg/cm^2 among the laser-cleaned sections. In general, all beam surfaces were considered clean for coating application with insignificant soluble chloride on the surface.

Table 11. Chloride Contamination on Laser-Cleaned 1-ft Beam Sections

Section	Surface Density, μg/cm^2
1A	0.4
2A	0.4
3	0.8
5	0.4
8	0.4
10	0.2
11	0.7
12	0.6
13	0.6
14	0.3
18[a]	0.5
19	0.4
Average (Laser ablated)	0.5

[a] Grit blasted.

Electrochemical Corrosion Testing

The electrochemical corrosion testing results from the Phase 5 work are shown in Tables 12 through 14. The electrochemical test results provide a qualitative comparison of the two cleaning methods. Laser-cleaned surfaces appeared to be electrochemically nobler than grit-cleaned surfaces. Of the two 5-ft beams, the corrosion potential of the grit-blasted steel was -617 mV vs. SSC (Ag/AgC$_l$) and that of the laser-cleaned steel was -580 mV vs. SSC (Ag/AgC$_l$) reference electrode, as shown in Tables 12 and 13. The corrosion rates among the laser-cleaned

beam sections (the 5-ft beam in Table 13 and the 1-ft sections in Table 14) were similar; the grit-blasted steel had a significantly higher corrosion rate, as shown in Table 12.

Table 12. Electrochemical Testing Results From Grit-Blasted 5-Ft Beam

Location	Corrosion Rate, mpy	Polarization Resistance, ohms	Corrosion Potential, mV vs. SSC (Ag/AgCl)
Cell No. 1	40.7	24.8	-615.8
Cell No. 2	55.1	15.9	-609.4
Cell No. 3	32.2	27.0	-614.0
Cell No. 4	39.8	21.4	-616.5
Cell No. 3	38.4	29.8	-620.2
Cell No. 5	46.3	18.4	-624.9
Average	42.1	22.9	-616.8
Max.	55.1	29.8	-609.4
Min.	32.2	15.9	-624.9
Standard Deviation	7.8	5.3	5.3

Table 13. Electrochemical Testing Results From Laser-Cleaned 5-Ft Beam

Location	Corrosion Rate, mpy	Polarization Resistance, ohms	Corrosion Potential, mV vs. SSC (Ag/AgCl)
Cell No. 1	35.5	24.8	-548.2
Cell No. 2	16.9	61.6	-568.8
Cell No. 3	6.9	122.6	-580.3
Cell No. 4	5.3	156.7	-607.7
Cell No. 5	9.6	136.2	-594.5
Average	14.9	100.4	-579.9
Max.	35.5	156.7	-548.2
Min.	5.3	24.8	-607.7
Standard Deviation	12.4	55.2	23.0

Table 14. Electrochemical Testing Results From 1-Ft Beams (Second Set Specimens)

Section ID	Corrosion Rate, mpy	Polarization Resistance, ohms	Corrosion Potential, mV vs. SSC (Ag/AgCl)
VDOT No. 1A	1.1	721.0	-336.6
VDOT No. 2A	1.7	477.8	-530.0
VDOT No. 3	1.1	763.3	-544.0
VDOT No. 5	30.5	39.1	-566.9
VDOT No. 8	2.8	292.7	-267.0
VDOT No. 10	2.5	325.4	-574.7
VDOT No. 11	2.8	293.5	-582.4
VDOT No. 12	2.9	283.1	-524.2
VDOT No. 13	49.6	24.0	-459.5
VDOT No. 14	41.9	28.4	-599.0
VDOT No. 18[a]	6.2	132.2	-568.9
VDOT No. 19	1.8	460.1	-524.1
Average	12.6	337.1	-500.8
Max.	49.6	763.3	-267.0
Min.	1.1	24.0	-599.0
Standard Deviation	18.5	255.5	106.4

[a] No. 18 was grit blasted; the rest were laser ablated.

From the cells on the grit-blasted 5-ft beam, the mean corrosion rate was 42.083 mils/year and the sample standard deviation was 7.818. From the cells on the laser-cleaned 5-ft beam, the mean corrosion rate was 14.840 mils/year and the sample standard deviation was 12.375. The t statistic that resulted from comparing the mean corrosion rates had a value of 7.356; the hypothesis that the mean corrosion rates are equal is rejected at a 4.3×10^{-5} level of confidence; LACR-cleaned steel appeared to have a lower corrosion rate.

From the cells on the grit-blasted 5-ft beam, the mean polarization resistance was 22.883 ohms and the sample standard deviation was 5.283. From the cells on the laser-cleaned 5-ft beam, the mean polarization resistance was 100.380 ohms and the sample standard deviation was 55.147 ohms. The t statistic that resulted from comparison of the mean polarization resistances had a value of -5.716. The hypothesis that the mean polarization resistances are equal is rejected at a 0.0043% level of confidence; the LACR-cleaned steel appeared to have a higher resistance to polarization.

From the cells on the grit-blasted 5-ft beam, the mean corrosion potential was -616.8 mV and the sample standard deviation was 5.308. From the cells on the laser-cleaned 5-ft beam, the mean corrosion potential was -579.9 mV and the sample standard deviation was 22.991. The t statistic that resulted from comparison of the mean corrosion potentials had a value of -6.358. The hypothesis that the mean corrosion potentials are equal is rejected at a 1.3×10^{-4} level of confidence; LACR-cleaned steel appeared to have a lower corrosion potential.

Coating Assessment of Treated Panels

Figure 44 shows examples of the panels after the coatings were fully cured. The DFT of each coating system is shown in Table 15. The surface cleaning method did not appear to influence the DFT.

Cyclic Exposure of Coated Steel Panels

To characterize the behavior of the coated panels, cyclic exposure tests were performed. They are the basis for quantitative evaluation of the performance of the coating systems as the coating panels go through cyclic testing conditions. These performance-related factors include adhesion, color, gloss, and rust creepage. It is worth noting that all four of the coatings measured are designed to be primer coats. As such, they would not normally be exposed to this level of exposure without having one or more finish coats over them. Photographs of the coated panels after 14 ALT cycles are shown in Figures 45 through 48.

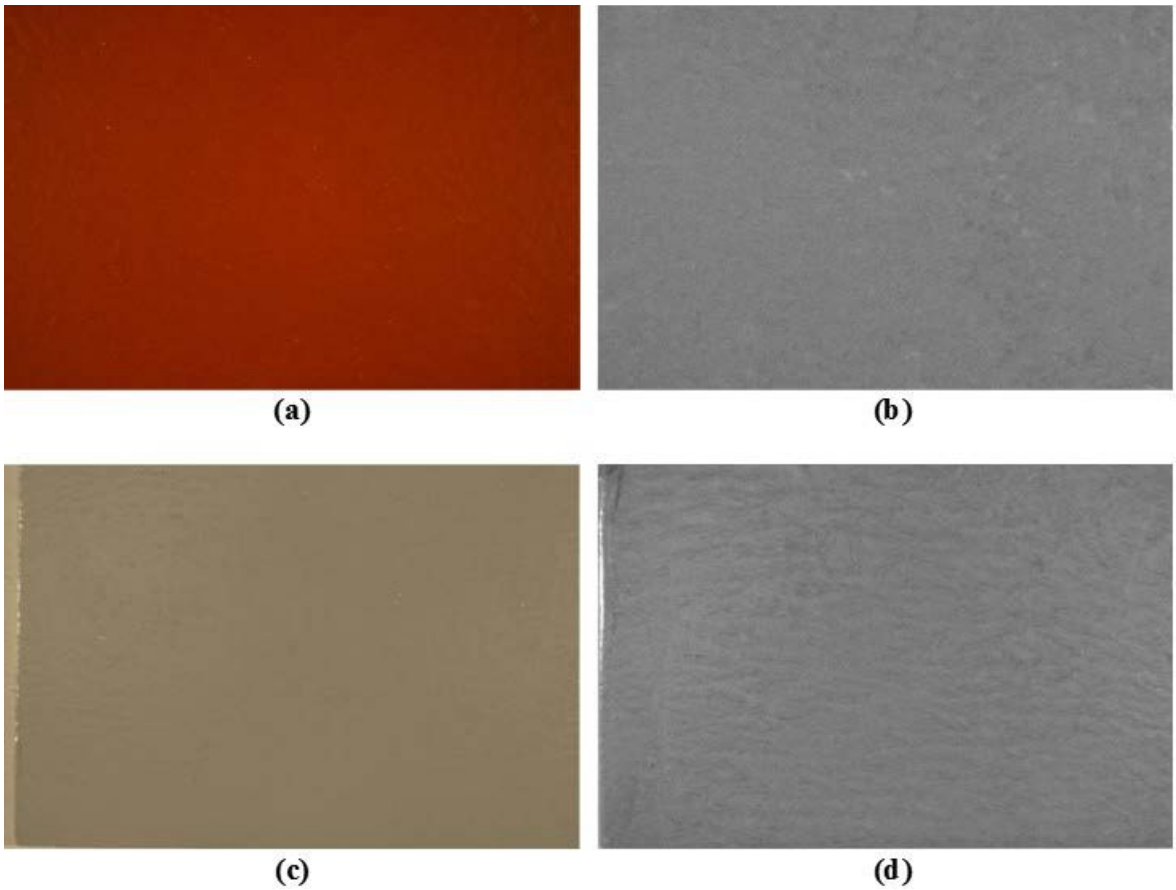

Figure 44. Images of Each Coating Tested on One of the Coated Panels: (a) Steel Spec Epoxy Primer; (b) flake filled epoxy; (c) phenalkamine epoxy; (d) epoxy mastic

Table 15. Dry Film Thickness for Coatings Applied To Grit-Blasted or Laser-Ablated Substrate

Coating	Substrate	Average Thickness, mil
Steel Spec Epoxy Primer	Grit blasted	7.8
	Laser ablated	7.7
Flake filled epoxy	Grit blasted	10.3
	Laser ablated	10.3
Phenalkamine epoxy (Carbogard 690)	Grit blasted	5.9
	Laser ablated	6.3
Epoxy mastic (Carbomastic 15)	Grit blasted	12.8
	Laser ablated	12.2

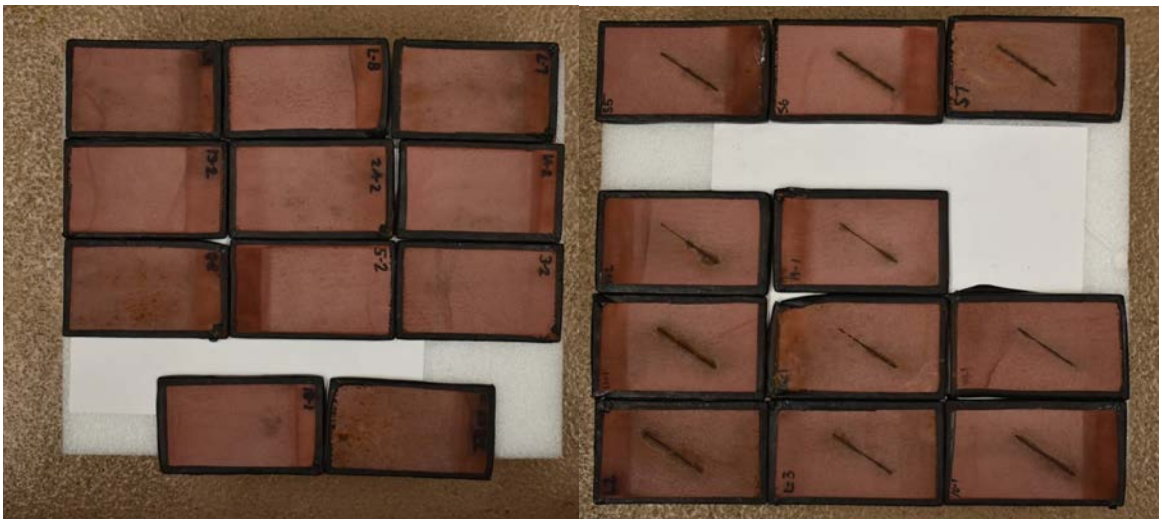

Figure 45. Panels Coated With Steel Spec Epoxy Primer. Grit-blasted panels are in upper row, and laser-ablated panels are in lower group.

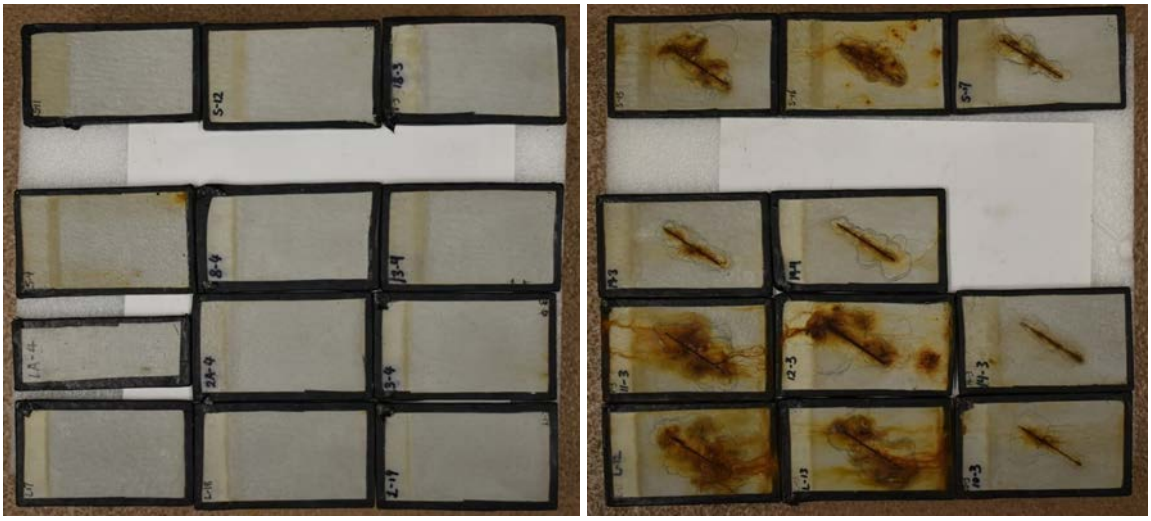

Figure 46. Panels Coated With Flake Filled Epoxy. Grit-blasted panels are in upper row, and laser-ablated panels are in lower group.

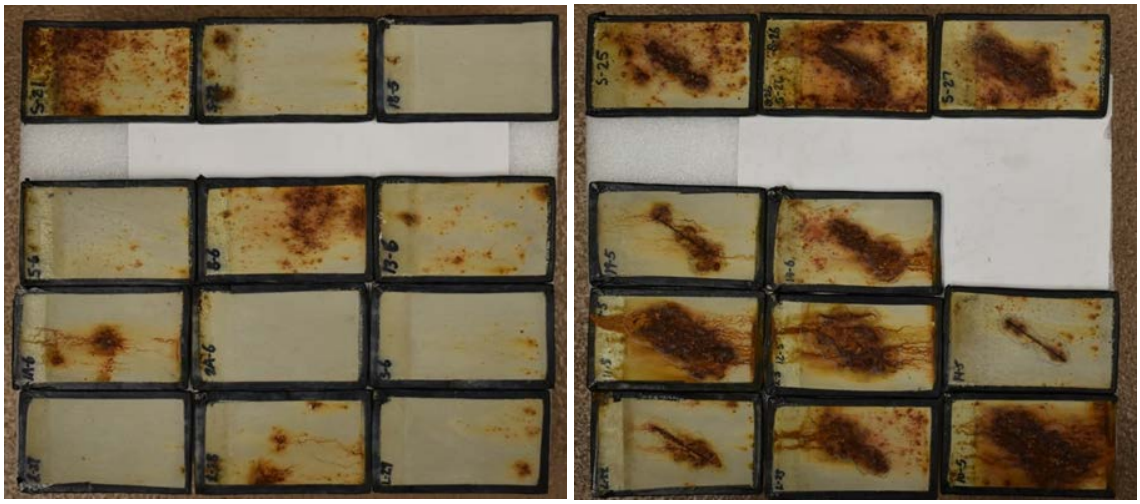

Figure 47. Panels Coated With Phenalkamine Epoxy. Grit-blasted panels are in upper row, and laser-ablated panels are in lower group.

Figure 48. Panels Coated With Epoxy Mastic. Grit-blasted panels are in upper row, and laser-ablated panels are in lower group.

Effect of Surface Treatment on Coating Adhesion Strength

The initial pull-off strength was tested after the coatings were fully cured, and the results are shown in Figure 49. From each coating system, three panels with grit-blasted substrate and nine panels with laser-cleaned surfaces were selected for the pull-off test. Three dollies were mounted on each panel. The average pull-off strength is reported in the figure.

After the coated panels were exposed to 14 ALT cycles, the pull-off test was performed again; the results are shown in Figure 50. Some panels had severe coating damage, and there was only enough surface area to mount one or two dollies. For each coating system, three panels with grit-blasted substrate (except for the Steel Spec Epoxy Primer coating system, which has two panels available) and nine panels with laser-cleaned surfaces were selected for pull-off testing.

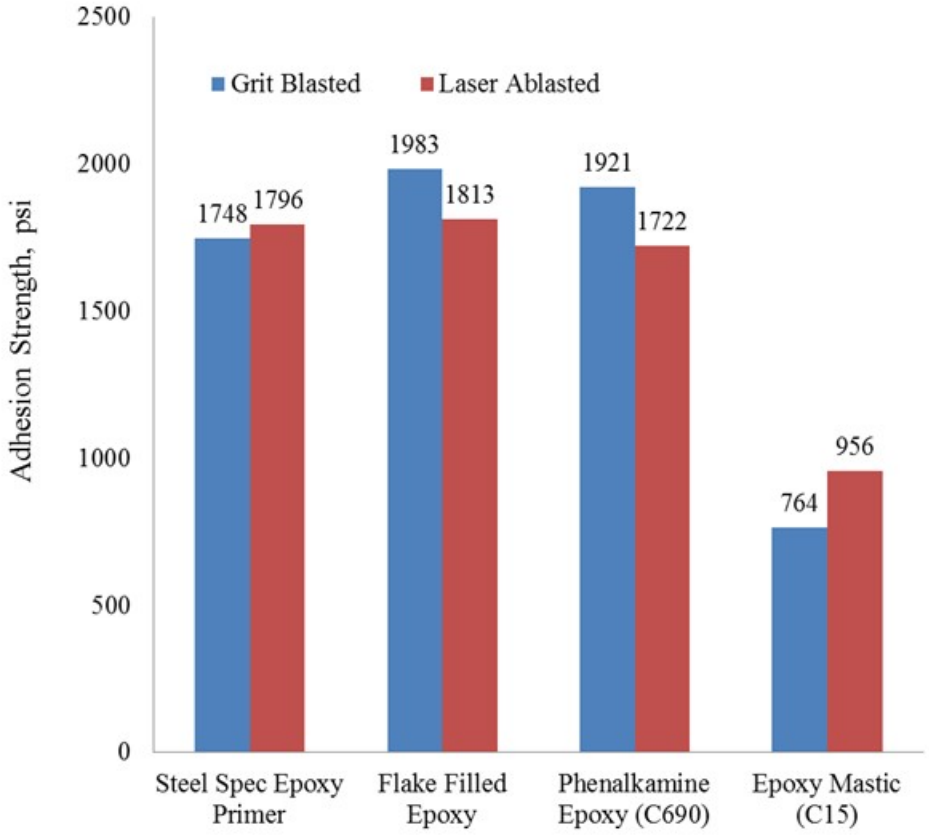

Figure 49. Initial Pull-Off Test Results

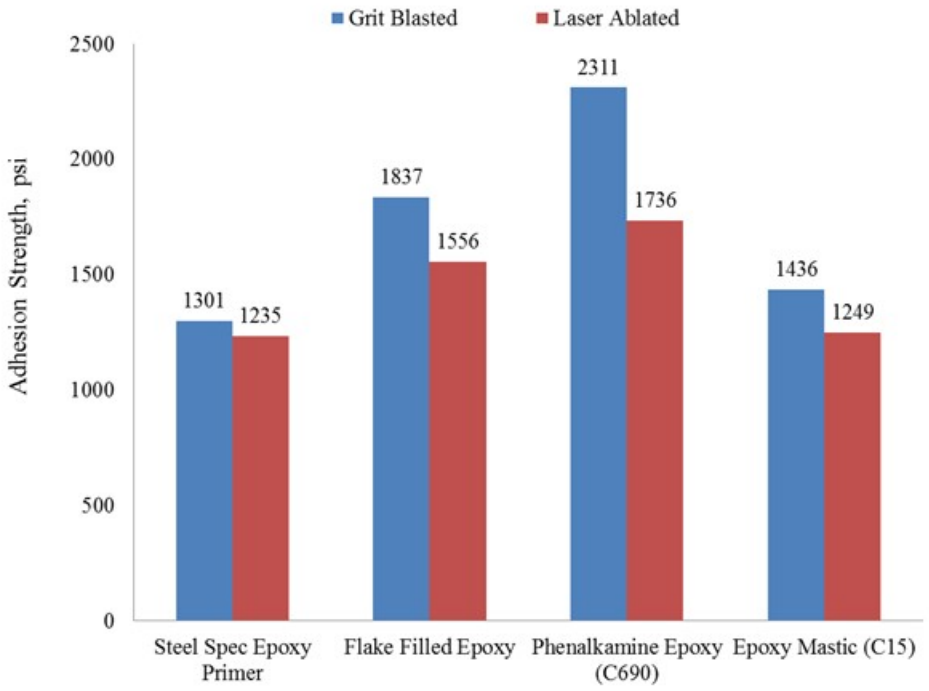

Figure 50. Pull-Off Test Results After 14 ALT Cycles. ALT = accelerated laboratory testing.

The voluminous raw pull-off test data that support Figures 49 and 50 are available from the authors upon request. Statistical comparisons of the mean pull-off strengths of each coating on laser-cleaned steel and grit-blasted steel, obtained from the raw data, are mixed.

Steel Spec Epoxy Primer, flake filled epoxy, and epoxy mastic at 3/8-in thickness had a statistically significant higher initial pull-off strength on the laser-cleaned steel substrates; flake filled epoxy at ¼-in thickness and phenalkamine epoxy at 3/8-in thickness had a statistically significant higher initial pull-off strength on the grit-blasted steel substrates. Flake filled epoxy at 3/8-in thickness had a statistically significant higher pull-off strength on the laser-cleaned steel substrates after 14 ALT cycles. Steel Spec Epoxy Primer, phenalkamine epoxy, and epoxy mastic at 3/8-in thickness had a statistically significant higher pull-off strength on the grit-blasted steel substrates after 14 ALT cycles, as did flake filled epoxy and phenalkamine epoxy at ¼-in thickness.

After the cyclic testing, the majority of the pull-off failure occurred because of cohesion failure of the coating film. The adhesion strength between the coating and the substrate could not accurately be determined by the data. It is worth noting, however, that the surface cleaning methods did not seem to affect the adhesion strength differently. Based on this work, it was concluded that there was little variation in the adhesion strength between the two surface cleaning methods.

Effect of Surface Treatment on Coating Specular Gloss

Gloss is the perception of a shiny surface by human eyes. Specular gloss compares the luminous reflectance of a test specimen to that of a standard specimen under the same geometric condition. Measurements by this test method correlate with visual observations of surface shininess made roughly at the corresponding angles. Measured gloss ratings are obtained by comparing the specular reflectance from the specimen to that from a black glass standard. The measured gloss ratings change as the surface refractive index changes because specular reflectance depends on the surface refractive index of the specimen.

A comparison between the grit-blasted and laser-ablation coated surfaces, before and after ALT, is provided in Table 16. The surface cleaning methods did not affect the trend in the gloss measurements for the four coatings studied.

Table 16. Gloss Measurements

Coating	Surface Preparation	Original Gloss		Cycle 14			
				Gloss		Gloss Reduction	
		20°	60°	20°	60°	20°	60°
Steel Spec Epoxy Primer	Grit blasting	0.2	1.0	0.3	0.9	52%	-15%
	Laser ablation	0.2	1.1	0.3	1.0	88%	-7%
Flake filled epoxy	Grit blasting	1.8	13.3	1.1	2.6	-41%	-81%
	Laser ablation	1.9	14.3	1.0	2.5	-47%	-82%
Phenalkamine epoxy (Carbogard 690)	Grit blasting	2.62	15.12	0.65	1.57	-75%	-90%
	Laser ablation	2.76	15.85	0.70	1.70	-75%	-89%
Epoxy mastic (Carbomastic 15)	Grit blasting	3.54	18.40	0.52	1.40	-85%	-92%
	Laser ablation	3.90	19.50	0.53	1.39	-86%	-93%

Effect of Surface Treatment on Coating Color

A comparison between the color measurements of the grit-blasted and laser-ablation coated surfaces, before and after ALT, is provided in Table 17. The surface cleaning methods did not affect the trend in the color for the four coatings studied.

Table 17. Color Measurements

Coating System	Surface Preparation	Original			Cycle 14						
		L*	a*	b*	L*	a*	b*	ΔL*	Δa*	Δb*	ΔE
Steel Spec Epoxy Primer	Grit blasting	31.92	18.47	11.78	44.06	14.25	11.60	12.14	-4.22	-0.18	12.9
	Laser ablation	31.81	18.26	11.71	46.60	14.90	10.26	14.80	-3.36	-1.45	15.2
Flake filled epoxy	Grit blasting	64.08	0.37	-0.62	67.88	-0.09	4.22	3.80	-0.45	4.84	6.2
	Laser ablation	64.06	0.37	-0.64	67.67	-0.25	4.29	3.61	-0.63	4.93	6.1
Phenalkamine epoxy (Carbogard 690)	Grit blasting	69.64	-0.98	4.41	66.75	3.51	16.08	-2.89	4.49	11.67	12.8
	Laser ablation	69.64	-1.02	4.42	70.27	0.42	10.01	0.64	1.44	5.59	5.8
Epoxy mastic (Carbomastic 15)	Grit blasting	56.04	-0.68	0.63	61.70	-0.64	5.29	5.67	0.04	4.66	7.3
	Laser ablation	56.44	-0.62	0.67	61.88	-0.92	5.43	5.45	-0.30	4.76	7.2

Rust Creepage Testing

Mean creepage distance was reported as the nominal creepage for the coating system, as shown in Figure 51. Based on these data, the use of laser ablation does not affect rust creepage development any differently than the use of the grit blasting surface preparation method.

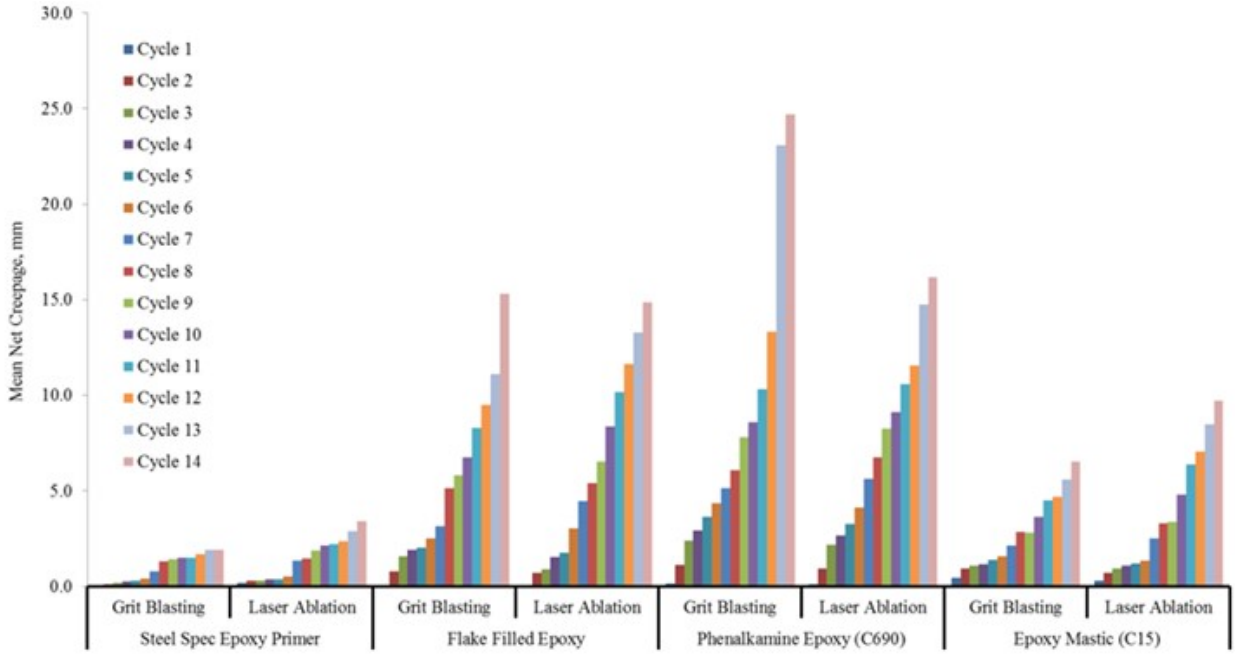

Figure 51. Rust Creepage Development on Scribed Panels

Additional Technologies for Coating Removal

Adjustable LACR Processing Head

A second LACR device with considerable promise was discovered late in the study. Powerlase Inc. was pursued for a demonstration of their high-power system that allows for 1.6KW of laser energy coupled into a small footprint with a 90 degree head design (Figure 52). Because of the proprietor's contractual requirements and scheduling issues with a U.K.-based location, the investigators were not able to conduct a demonstration in person on comparable materials of interest to VDOT. The design of the Powerlase laser head system is of significant interest because of both its geometry and lightweight design, combined with a higher energy laser source.

Figure 52. Demonstration of Powerlase 1.6 kW Vulcan Laser Head in Operation. Note compact and lightweight design.

Induction Coating Removal

In addition to LACR, induction coating removal (ICR) is another viable coating removal technology. As implied by the name, ICR operates on the principle of electromagnetic induction, where heat is generated in the near surface of the steel substrate (~0.3 mm), which subsequently breaks the bonds between the substrate and coating layer without dissociation or complete disintegration of the coating system. Using a hand-operated induction coil, a high frequency alternating current is placed close to the coating and substrate, in turn creating electron eddy currents within the steel substrate that causes the metal to heat up rapidly. Figure 53 shows a diagram of how this technology is used to remove coatings from steel. Although the fundamental operating principle behind ICR is different from that behind LACR, the ICR process has additional benefits beyond the LACR process, which include the following:

- minimal VOC production
- minimal waste production
- minimal consumables, high removal rate, and small-scale equipment with nominal power requirements.

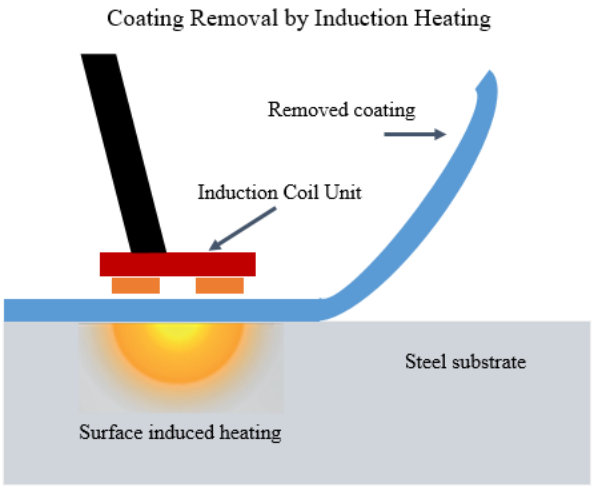

Figure 53. Induction Coating Removal Diagram Showing How Heat Provided By an Induction Coil Is Used to Heat Rapidly and Locally the Steel Substrate Causing the Coating to Disband From the Steel Surface

The major distinction between LACR and ICR is the final substrate appearance. LACR results in a substrate with a clean appearance, with coatings, rust, and other contaminants on the substrate surface removed. In comparison, ICR removes the bulk coating layer, potentially leaving behind levels of residual rust, primer layers, or adhesives. A proposed two-step method of ICR is (1) remove the coating system rapidly, and (2) then consider using LACR. Because of contractual and scheduling constraints, ICR was never tested in this study. Two companies that make ICR equipment are RPR Technologies and EFD Induction. Each company produces hand-held portable systems for on-site coating removal operations.

Cost-Comparison Scenarios and Data Needs

The most likely applications envisioned for LACR are (1) cleaning of beam ends or limited zones of a substructure threatened by corrosion prior to repainting, and (2) removal of paint from small portions of beams or other steel members prior to hot work such as grinding or torch cutting.

It is conceivable that ICR will be a cost-competitive alternative for removing coatings from an entire steel substructure.

Likely Scenarios

At present, VDOT seldom performs beam-end recoating or zone recoating because localized coating removal is uneconomical. The state of the practice for removing old layers of primer and paint is abrasive blasting. The time and resource cost of setting up a work site for environmental containment during abrasive blasting of a small surface area is nearly the same as the cost of setting up for blasting of an entire substructure. LACR appears to offer a means of removing paint on a small area at a small environmental containment cost, making economical a localized recoating that heretofore was uneconomical.

At present, VDOT typically performs hot work on steel without prior removal of the paint or else removes the paint locally by grinding without environmental containment. The amount of heavy metals liberated during a small area job is modest and, as noted previously, containment incurs a large, relatively fixed cost. LACR appears to offer a means of avoiding operator exposure to heavy metals during hot work at a small environmental containment cost.

Available Cost Pieces and Missing Cost Pieces

The laser ablation units operated in this this have an up-front acquisition cost on the order of $500,000. To make a cost comparison between the two alternatives, i.e., abrasive blasting and LACR, on a real or stylized hypothetical bridge recoating job would require a certain number of assumptions and cost estimates: (1) a specification of the parameters of the job, such as the number of square feet of surface to be cleaned, the number of linear feet of corner (intersection of two faces) to be cleaned, and the number of corners (intersection of three faces) to be cleaned and their position on the deck; (2) the time and resource costs involved in setting up (and taking down) the required environmental containment and workplace safety measures; (3) the time and resource costs involved in carrying out the coating removal; and (4) the time and resource costs involved in disposing of waste created during the operation.

Cost estimates for the baseline alternative, abrasive blasting, are available at present. An analysis of a set of 31 spot coating contracts from 2012 found that each such job incurred an average painting cost of $1,672,786 (contract item code 68455); an average environmental protection cost of $1,390,827 (contract item codes 68747 and 68476); and an average materials disposal cost of $105,548 (contract item codes 68490 and 6892).[1] An analysis of a subset of 15 of these 31 contracts found that the average price amounted to about $65 per square foot.

This study has determined some limits to the amount of environmental containment that laser ablation will require. It has also produced some observations concerning the cost and speed of operating a laser ablation unit. A big missing piece in the cost comparison is the cost of waste disposal after LACR. All findings in this study indicated that the four filters in the laser ablation unit captured most of the contaminants in the paint and other coatings as they were removed from the steel surface. For reasons of time limitations, however, as well as for reasons of caution, in the laboratory and field demonstrations, a laser unit was not operated up to the point at which the contaminants in the paint "broke through" one or more of the four filters. Some quantification of the filters' capacity during removal of common surface coatings is needed in order to estimate the frequency with which the filters will be changed during the ongoing operation of a laser unit.

CONCLUSIONS

Coating Removal and Recoating

- *LACR effectively removes the coatings investigated, including lead-based alkyd paints*. As was observed by previous researchers and the current researchers for a previous investigation of a particular epoxy-based coating, LACR can effectively remove coatings from steel

substrates. The steel used in this study included legacy components, which were never subjected to abrasive blasting prior to their original coating application. LACR was successful in removing coatings from steel with mill scale (oxide from the manufacturing process), although the substrate of the microscopic surface detail is distinct. Further, although microscopic investigation revealed that small coating particles remained on the surface after cleaning (which are unapparent to the naked eye), these particles did not adversely affect subsequent coating adhesion.

- *LACR does not detrimentally affect the mechanical properties or chemical composition of the steel* (A36 structural steel) that was examined in this study despite the fact that microscopic investigation revealed very local (~1 μm thick) surface melting of the metal substrate (or the oxide that covers it); measurements of the hardness revealed no degradation relative to the interior; and the tensile yield strength, ultimate strength, ductility, fatigue strength, and chemical composition were all on parity with expected values of A36 steel.

- *The coating adhesion of LACR surfaces is satisfactory*, with adhesion testing revealing an average initial pull-off strength of approximately 1,800 psi when an epoxy binder was used for recoating. The adhesion on a laser-cleaned surface was not consistently superior to the adhesion on a grit-blasted surface. However, electrochemical test results indicated that the LACR surface was relatively nobler than the grit-blasted surface. Coating color, gloss, and rust creepage were similar when LACR-cleaned surfaces and grit-blasted surfaces were compared.

Industrial Hygiene

- *As shown by the IH study, the engineering controls associated with LACR are effective in maintaining potential exposures for the laser operator below the current OSHA PEL and OSHA AL.* Of particular interest to this study was the detection of lead. The highest operator lead level observed was 4.3 $\mu g/m^3$, which is below the AL (30 $\mu g/m^3$) and PEL (50 $\mu g/m^3$) for lead. This contrasts by nearly 4 orders of magnitude with the lead level observed during a comparable grit-blasting operation. The results of the IH study showed that LACR provides a potential cost benefit, since it does not require the type of containment that traditional grit-blasting approaches require. It is noted that this LACR system's particle filtration system must be disposed of as hazardous waste and that appropriate personal protective equipment should be worn during the removal of the filter for disposal. Although exposure was evaluated during LACR operation, further personal monitoring during disposal of the filters is required to determine employee exposure levels.

- *LACR can be employed as a lead removal technique in preparation for other processes, such as cutting, grinding, or welding, which are widely used by VDOT.* Comparison of lead levels in the personal air samples of operators engaged in grinding and in oxyacetylene torch cutting indicated that whereas hot work performed on painted steel creates a hazardous lead concentration in the breathing air of the operator many times in excess of regulatory limits, hot work on steel that has been cleaned in advance by LACR creates a lead concentration unlikely to cause exposure above regulatory limits when completed under normal operating

conditions, typically 3 hours or less. LACR on the rolled I-beam showed the greatest reduction in lead while doing hot work when compared to the welded C-channel beam.

- *LACR will not remove coatings sandwiched between two steel surfaces.* The welded C-channel beam could not be cleaned effectively where the two channel surfaces made contact. This resulted in higher emissions during hot work that could cause exposure, but emissions were reduced greatly when compared to cutting through a fully coated beam.

Environmental Compliance

- *As shown by TCLP testing for Ag, As, Ba, Cd, Cr, Hg, Pb, and Se, some of the filters of the LACR system are considered regulatory hazardous waste.* During Phase 1, the particle debris filter was determined to be a regulatory hazardous waste for lead. During Phase 2, the HEPA filter exceeded the regulatory waste requirements for lead and the particle debris filter exceeded the regulatory waste requirements for lead and chromium. Therefore, these filters must be disposed of or cleaned using the proper personal protective equipment for handling hazardous waste. However, it is noted that in both cases the LACR unit was not run to the point that the filtering systems were saturated and the system such down or reached breakthrough. Accordingly, additional waste profiling of the HEPA and carbon filtering system components will be required as the LACR operation is scaled up.

Complementary Coating Removal Techniques

- *As shown by field studies, because of tight space limitations and geometry, removing coatings on bridge beam ends and bulk heads with the selected laser system is problematic.* This is unfortunate because present productivity rates do not warrant the use of this device for large area coating removal applications, rendering such niche applications attractive. The team did observe, although was unable to test in detail, alternative LACR systems that were smaller, lighter weight, and more powerful. Such characteristics could ameliorate concerns about productivity and tight space limitations.

- *Further investigation of LACR and ICR is warranted*. The manufacturers of other LACR systems boast higher productivity rates than that of the system presently considered because of higher laser power (1.6 kW versus 1 kW) and rapid, large area, wider interaction angles associated with the ICR systems. Further field testing will provide the operating cost data needed to make a complete cost comparison between LACR and current standard coating removal methods such as abrasive blasting.

RECOMMENDATIONS

1. *VDOT's Structure and Bridge Division should consider implementing the use of LACR for spot coating and beam-end repairs.*

2. *Using earlier work performed in this study, VDOT's Structure and Bridge Division developed guidance on using LACR to remove a bridge coating, including those containing lead, before performing hot work operations on coated steel. Upon completion of this coating removal study, VDOT's Structure and Bridge Division should continue with this course of action.*

3. *VTRC should work with VDOT's Structure and Bridge Division and a VDOT district to identify a bridge(s) requiring beam-end repairs and initiate an implementation project. During this project, VTRC would also work with VDOT's Environmental Division to evaluate and document the efficiency of the filter system and required disposal parameters.*

4. *VTRC should work with VDOT's Structure and Bridge Division and VDOT's Environmental Division to investigate the use of other LACR systems and the ICR techniques that might benefit VDOT.*

IMPLEMENTATION AND BENEFITS

Implementation

For Recommendation 1 and Recommendation 2, implementation would be similar. Both recommendations allow VDOT to use LACR where it is most needed. For Recommendation 1, this could be removing coatings near leaking bridge joints prior to making beam-end repairs. Generally, these repair locations are relatively small, with most of the steel beam still in good condition. For Recommendation 2, this could be the removal of older steel beams supporting bridges with a timber deck. Typically, these types of structures were constructed with coated rolled steel beams that might contain lead in the coating. Using LACR for both applications could be a more efficient way of dealing with the removal of smaller areas of coatings. Implementation of Recommendation 1 will occur within 3 years of the publication of this report. Recommendation 2 has already been implemented.

For Recommendation 3, VTRC will initiate an implementation project. VTRC will also form a task group to provide input and ensure the successful completion of this implementation project. The task group will include members from VDOT"s Structure and Bridge Division, VDOT's Environmental Division, a VDOT district, and VTRC. The task group will identify a candidate bridge (possibly multiple bridges) that would benefit from the use of LACR to remove coatings from beam ends. During this project, VTRC will work with VDOT's Environmental Division and the selected district to evaluate and document the efficiency of the filter system and required disposal parameters. VTRC will issue a report on the outcome of these efforts. Implementation of this recommendation will occur within 4 years of the publication of this report.

For Recommendation 4, VTRC will initiate a study by contracting with a university that has a history of work in this area. VTRC will also form a task group to provide guidance during the study and ensure the successful completion of the study. The task group will include members from VTRC, VDOT's Structure and Bridge Division, and VDOT's Environmental

Divisions. The task group will provide guidance to the university contractor as they investigate other LACR systems and the ICR technique for removing bridge coatings. VTRC will issue a report upon completion of this study. Implementation of this recommendation will occur within 4 years of the publication of this report.

Benefits

As noted previously, the most likely applications envisioned for LACR are (1) cleaning of beam ends or limited zones of a substructure threatened by corrosion, prior to repainting, and (2) removal of paint from small portions of beams or other steel members, prior to hot work such as grinding or torch cutting.

The up-front approximate acquisition cost of a laser ablation unit similar to the ones used in this study is known. Although zone recoating is uncommon, given the current technical options, costs for a few historical jobs using abrasive blasting are available. Although this study collected some data concerning the operating costs of laser ablation, certain pieces of information, for example, data bearing on the waste disposal costs, remained to be acquired.

Implementation of the study recommendations, which foresee trial applications of LACR for suitable field projects, is expected (1) to provide precise, realistic job parameters for a cost comparison; (2) to provide a realistic setting in which to record the cost of setting up environmental containment for LACR; (3) to corroborate (or revise) the operating cost and speed features reported here; and (4) to provide some data with which to model the service life of the filters in which the waste from the LACR process is collected.

ACKNOWLEDGMENTS

The authors are grateful for the support provided by VDOT; the Federal Highway Administration; VDOT's Structure and Bridge Division; VDOT's Environmental Division; VDOT's Materials Division; VDOT's Lynchburg, Culpeper, and Hampton Roads districts; and VTRC. Specifically, the contributions from Mary Bennett, George Fitch, C. Wayne Fleming, Rodolfo Maruri, Adam Matteo, Jeffery Milton, Raquel Rickard, Michael Sprinkel, David L. Wilson, and Kevin Wright are recognized.

REFERENCES

1. Sharp, S.R., Donaldson, B.M., Milton, J.L., and Fleming, C.W. *Preliminary Assessment of Procedures for Coating Steel Components on Virginia Bridges.* VCTIR 14-R1. Virginia Center for Transportation Innovation and Research, Charlottesville, 2013.

2. Castillejo, M. Analytical Study of the Chemical and Physical Changes Induced by Krf Laser Cleaning of Tempera Paints. *Analytical Chemistry,* Vol. 74, Issue 18, 2002, pp. 4662-4671.

3. de Cruz, A., Wolbarsht, M.L., and Hauger, S.A.. Laser Removal of Contaminants From Painted Surfaces. *Journal of Cultural Heritage,* Vol. 1, 2000, pp. S173-S180.

4. Maravelaki-Kalaitzaki, P., Zafiropulos, V., and Fotakis, C. Excimer Laser Cleaning of Encrustation on Pentelic Marble: Procedure and Evaluation of the Effects. *Surface Science,* Vol. 148.1-2, 1999, pp. 92-104.

5. Oujja, M., Rebollar, E., Castillejo, M., Domingo, C., Cirujano, C., and Guerra-Librero, F. Laser Cleaning of Terracotta Decorations of the Portal of Palos of the Cathedral of Seville. *Journal of Cultural Heritage,* Vol. 6, Issue 4, 2005, pp. 321-327.

6. Cooper, M.I., Emmony, D.C., and Larson, J. Characterization of Laser Cleaning of Limestone. *Optics & Laser Technology,* Vol. 27, Issue 1, 1995, pp. 69-73.

7. Siano, S. Laser Cleaning in Conservation of Stone, Metal, and Painted Artifacts: State of the Art and New Insights on the Use of the Nd:YAG Lasers. *Applied Physics A,* Vol. 106, Issue 2, 2012, pp. 419-446.

8. Salimbeni, R. Assessment of the State of Conservation of Stone Artworks After Laser Cleaning: Comparison With Conventional Cleaning Results on a Two-Decade Follow Up. *Journal of Cultural Heritage,* Vol. 1, Issue 4, 2000, pp. 385-391.

9. Liu, K., and Garmire, E. Paint Removal Using Lasers. *Applied Optics,* Vol. 34, Issue 21, 1995, pp. 4409-4415.

10. Delaporte, P., Gastauda, M., Marine, W., Sentis, M., Uteza, O., Thouvenot, P., Alcaraz, J.L., Le Samedy, J.M., and Blin, D. Dry Excimer Laser Cleaning Applied to Nuclear Decontamination. *Applied Surface Science,* Vols. 208-209, 2003, pp. 298-305.

11. Mateo, M.P., Ctvrtnickova, T., Fernandez, E., Ramos, J.A., Yanez, A., and Nicolas, G. Laser Cleaning of Varnishes and Contaminants on Brass. *Applied Surface Science,* Vol. 255, Issue 10, 2009, pp. 5579-583.

12. Daurelio, G., Chita, G., and Cinquepalmi, M. Laser Surface Cleaning, De-Rusting, De-Painting and De-Oxidizing. *Applied Physics A,* Vol. 69, Issue 1, 1999, pp. S543-S546.

13. Guan, Y.C. Laser Surface Cleaning of Carbonaceous Deposits on Diesel Engine Piston. *Applied Surface Science,* Vol. 270, 2013, pp. 526-530.

14. Airforce Technology. USAF's Travis AFB Tests Laser Technique to Remove Corrosion. March 15, 2018. www.airforce-technology.com/news/usafs-travis-afb-tests-laser-technique-remove-corrosion/. Accessed July 16, 2019.

15. Chen, G. X., Kwee, T. J., Tan, K. P., Choo, Y. S., and Hong, M. H. High-Power Fibre Laser Cleaning for Green Shipbuilding. *Journal of Laser Micro/Nanoengineering,* Vol. 7, No. 3, 2012, pp. 249-253.

16. Head, J.D., and Niedzielski, J. P. *Laser Paint Stripping*. Laser Technologies Inc., South Lyon, Mich., 1991.

17. D'Addona, D.M. Laser Ablation of Primer During the Welding Process of Iron Plate for Shipbuilding Industry. *Procedia Cirp,* Vol. 33, 2015, pp. 464-469.

18. Shamsujjoha, M., Brooks, J.R., Tyler, T.J., Jr., Agnew, S.R., and Fitz-Gerald. J.M. Effects of Laser Ablation Coating Removal (LACR) on a Steel Substrate: Part 1: Surface Profile, Microstructure, Hardness, and Adhesion. *Journal of Surface and Coatings Technology*, Vol. 281, 2015, pp. 193-205.

19. Shamsujjoha, M., Brooks, J.R., Tyler, Jr., T.J., Agnew, S.R., and Fitz-Gerald. J.M. Effects of Laser Ablation Coating Removal (LACR) on a Steel Substrate: Part 2: Residual Stress and Fatigue. *Journal of Surface and Coatings Technology,* Vol. 281, 2015, pp. 206-214.

20. Cargill, R.R. *Closed-Loop Laser Ablation for Navy Maintenance Applications*. ASNE 2011 Symposium, 2011. www.lasertronics.com/wp/wp-content/uploads/2011/10/ASNE-2011-Symposium-Paper.pdf. Accessed May 2018.

21. EverGreene Architectural Arts. *U.S. Capitol North Wing.* Washington, D.C. https://evergreene.com/projects/laser-cleaning-of-marble-at-the-us-capitol-north-wing/. Accessed May 15, 2018.

22. Public Services and Procurement Canada. *How Parliamentary Buildings Are Rehabilitated*. Ottawa, Ontario. https://www.tpsgc-pwgsc.gc.ca/citeparlementaire-parliamentaryprecinct/rehabilitation/parlement-parliamentary-eng.html. Accessed July 17, 2019.

23. Virginia Department of Transportation. *Industrial Hygiene Survey Report: Norton Sandblasting Laser Ablation.* Richmond, 2018.

24. ASTM International. ASTM E8 / E8M-16a: Standard Test Methods for Tension Testing of Metallic Materials. In *Annual Book of ASTM Standards, Volume 03.01*. West Conshohocken, Penn., 2016.

25. ASTM International. ASTM D4417-14: Standard Test Methods for Field Measurement of Surface Profile of Blast Cleaned Steel. In *Annual Book of ASTM Standards, Volume 06.02.* West Conshohocken, Penn., 2014.

26. The Society for Protective Coatings. *Field Methods for Extraction and Analysis of Soluble Salts on Steel and Other Nonporous Substrates.* SSPC Technology Guide 15. Pittsburgh, Penn., 2013.

27. Chlor*Rid International, Inc. CHLOR*TEST "CSN"™. http://www.chlor-rid.com/testkits/chlortestCSN.php. Accessed November 1, 2018.

28. The Society for Protective Coatings. *SSPC-PA2: Determining Compliance to Required DFT.* Pittsburgh, Penn., 2018.

29. ASTM International. ASTM D7091-13: Standard Practice For Nondestructive Measurement of Dry Film Thickness of Nonmagnetic Coatings Applied to Ferrous Metals and Nonmagnetic, Nonconductive Coatings Applied to Non-Ferrous Metals. In *Annual Book of ASTM Standards, Volume 06.01*. West Conshohocken, Penn., 2013.

30. ASTM International. ASTM D5894-16: Standard Practice for Cyclic Salt Fog/UV Exposure of Painted Metal (Alternating Exposures in a Fog/Dry Cabinet and a UV/Condensation Cabinet). In *Annual Book of ASTM Standards, Volume 06.01*. West Conshohocken, Penn., 2016.

31. ASTM International. ASTM D4541-09: Standard Test Method for Pull-Off Strength of Coatings Using Portable Adhesion Testers. In *Annual Book of ASTM Standards, Volume 06.02*. West Conshohocken, Penn., 2010.

32. ASTM International. ASTM D5230-08: Standard Test Method for Specular Gloss. In *Annual Book of ASTM Standards, Volume 06.01*. West Conshohocken, Penn., 2010.

33. ASTM International. ASTM D2244-09A: Standard Practice for Calculation of Color Tolerances and Color Differences from Instrumentally Measured Color Coordinates. In *Annual Book of ASTM Standards, Volume 06.01*. West Conshohocken, Penn., 2010.

34. ASTM International. ASTM D7087-05A: Standard Test Method for an Imaging Technique to Measure Rust Creepage at Scribe on Coated Test Panels Subjected to Corrosive Environments. In *Annual Book of ASTM Standards, Volume 06.01*. West Conshohocken, Penn., 2010.

35. Baὶuerle, D. *Laser Processing and Chemistry,* 4th ed. Springer, Heidelberg, Germany, 2011.

36. Razab, M.K.A.A., Noor, A.M., Jaafar, M.S., Abdullah, N.H., Suhaimi, F.M., Mohamed, M., Adam, N., and Yusuf, N.A.A.N. A Review of Incorporating Nd:YAG Laser Cleaning Principal in Automotive Industry. *Journal of Radiation Research and Applied Sciences,* Vol. 11, 2018, pp. 393-402.

37. Toftmann, B., Papantonakis, M.R., Auyeung, R.C.Y., Kim, W., O'Malley, S.M., Bubb, D.M., Horwitz, J.S., Schou, J., Johansen, P.M., Haglun Jr., R.F. UV and RIR Matrix Assisted Pulsed Laser Deposition of Organic MEH-PPV Films. *Thin Solid Films,* Vol. 453, 2004, pp. 177-181.

38. Mercado, A.L., Allmond, C.E., Hoekstra, J.G., and Fitz-Gerald, J.M. Pulsed Laser Deposition vs. Matrix Assisted Pulsed Laser Evaporation for Growth of Biodegradable Polymer Thin Films. *Applied Physics A,* Vol. 81, Issue 3, 2005, pp. 591-599.

39. Forrest, S.R. The Path to Ubiquitous and Low-Cost Organic Electronic Appliances on Plastic. *Nature,* Vol. 428.6986, 2004, p. 911.

40. Hohnholz, D., Okuzaki, H., and MacDiarmid, A.G. Plastic Electronic Devices Through Line Patterning Of Conducting Polymers. *Advanced Functional Materials,* Vol. 15, Issue 1, 2005, pp. 51-56.

41. Romoli, L., Tantussi, G., and Dini, G. Experimental Approach to the Laser Machining Of PMMA Substrates for the Fabrication of Microfluidic Devices. *Optics and Lasers in Engineering,* Vol. 49, Issue 3, 2011, pp. 419-427.

42. Liu, H.-B., and Gong, H.-Q. Templateless Prototyping of Polydimethylsiloxane Microfluidic Structures Using a Pulsed CO_2 Laser. *Journal of Micromechanics and Microengineering,* Vol. 19, Issue 3, 2009, p. 037002.

43. Moreira, G.E.F., Tomazelli Coltro, W.K., and Garcia, C.D. Fast and Versatile Fabrication of PMMA Microchip Electrophoretic Devices by Laser Engraving. *Electrophoresis,* Vol. 35, Issue 16, 2014, pp. 2325-2332.

44. Trokel, S.L., Srinivasan, R., and Braren, B. Excimer Laser Surgery of the Cornea. *American Journal of Ophthalmology,* Vol. 96, Issue 6, 1983, pp. 710-715.

45. Jako, G.J. Laser Surgery of the Vocal Cords: An Experimental Study With Carbon Dioxide Lasers on Dogs. *The Laryngoscope,* Vol. 82, Issue 12, 1972, pp. 2204-2216.

46. Srinivasan, R., and Braren, B. Ultraviolet Laser Ablation of Organic Polymers. *Chemical Reviews,* Vol. 89, Issue 6, 1989, pp. 1303-1316.

47. Bityurin, N., Luk'yanchuk, B.S., Hong, M.H., and Chong, T.C. Models for Laser Ablation of Polymers. *Chemical Reviews,* Vol. 103, Issue 2, 2003, pp. 519-552.

48. Madhukar, Y.K., Mullick, S., Shukla, D.K., Kumar, S., and Nath, A.K. Effect of Laser Operating Mode in Paint Removal With a Fiber Laser. *Applied Surface Science,* Vol. 264, 2013, pp. 892-901.

49. Pyć, W.A. *Field Performance of Epoxy-Coated Reinforcing Steel in Virginia Bridge Decks.* Virginia Polytechnic Institute and State University, Blacksburg, 1998.

50. Vaca-Cortes, E., Lorenzo, M.A., Jirsa, J.O., Wheat, H.G., and Carrasquillo, R.L. *Adhesion Testing of Epoxy Coating.* Research Report No. 1265-6. The University of Texas at Austin, 1998.

51. Toubia, E., and Emami, S. *Performance Comparison of Structural Steel Coating Systems*. FHWA/OH-2016/8. Ohio Department of Transportation, Columbus, 2016.

52. Transportation Research Board. *Successful Preservation Practices for Steel Bridge Coatings*. NCHRP Project 20 68A, Scan 15-03. Washington, D.C., 2016.

53. Petrie, E.M. Adhesion & Bonding. *Metal Finishing,* Vol. 107, No. 10, 2009, pp. 48-50.

54. Fleming, C.W. Personal Communication, 2017.

55. Lambourne, R., and Strivens, T.A., Eds. *Paint and Surface Coatings: Theory and Practice*. Woodhead Publishing, Sawston, Cambridge, U.K., 1999.

56. Sunkara, V., and Cho, Y.-K. Investigation on the Mechanism of Aminosilane-Mediated Bonding of Thermoplastics and Poly(Dimethylsiloxane). *ACS Applied Materials & Interfaces,* Vol. 4, No. 12, 2012, pp. 6537-6544.

57. Momber, A.W., Koller, S., and Dittmers, H.J. Effects of Surface Preparation Methods on Adhesion of Organic Coatings to Steel Substrates. *Journal of Protective Coatings and Linings,* Vol. 21, Issue 11, 2004, pp. 44-50.

58. ASTM International. ASTM A36/A36M-14: Standard Specification for Carbon Structural Steel. In *Annual Book of ASTM Standards, Volume 01.04*. West Conshohocken, Penn., 2014.

59. Ruben, P.M. *Study of the Fatigue Strength in the Gigacycle Regime of Metallic Alloys Used In Aeronautics and Off-Shore Industries*. Mechanics of Materials [physics.class-ph]. Arts et Métiers ParisTech, Paris, France, 2010.

60. Shamsujjoha, M. *The Effects of Laser Ablation Coating Removal on the Fatigue Performance of a High Strength Structural Steel.* Doctoral Dissertation. University of Virginia, Charlottesville, 2017.